Reviewer # 1 suggestions and author response

General comment

Andela et al., present a novel and very important dataset of several important fire characteristics globally on a daily basis. This dataset will serve earth system and social scientists on topics ranging from (but not limited to) fire emission estimates in earth system modelling, feedback between fires and ecosystem, fire management and studies of socio-economic feedback of fires. The manuscript is well written and the underlying methodologies have been explained precisely. Being the first dataset of such kind, a complete validation was challenging. However the authors have used the available resources, e.g. VIIRS (globally for four different ecosystems) for burn date, MTBS in the US for the fire perimeter and a combination of both for the fire duration.

The dataset, however, has a large uncertainty for short fires (persisting for less than a day, for example, crop residue fires), which is acknowledged in the discussion. I have only minor comments regarding this manuscript and recommend publication of this manuscript in ESSD after the authors have addressed them:

We thank the reviewer for his/her constructive comments and thoughtful review. Please find our detailed response along with the suggested changes to our manuscript below. Note that we will upload the updated manuscript using track change (in response to both reviews) in a separate post.

Specific comments:

The methodology considers clusters of fires in a given fire season (12 months) as a starting point. What if the fires season is less than 12 months? For example, the same area is burnt twice after a gap of six months? As per my understanding, the local minima filter will only assign it to the later burnt date of the fire season. This will also have consequences on the estimation of fire duration and perimeter.

This is correct, we try to minimize the amount of pixels that burned twice during a single burning season by defining the burning season as "5 months before until 6 months after the month of maximum mean burned area" for each individual 10° x 10° MODIS tile. In most of the world (particularly areas that burn frequently) the fire season is quite clearly defined, e.g. wet and dry seasons in the tropics or cold winters and warm summers at higher latitudes; however, in regions without clear seasonality (e.g. always dry or wet), or some areas with both natural and cropland fires, our methodology is not ideal. In case there was overlap between two burning events we only retain the earliest burn dates. Therefore, a small fraction (<1%) of global burned area is effectively removed from our dataset, indeed affecting fire perimeters by reducing overall burned area. The advantage of our methodology is that we can produce user friendly global "annual" layers of fire behavior, both gridded at 500-m resolution, as well as in the form of shapefiles.

In response to this suggestion will more clearly explain these tradeoffs. In particular, we will rephrase lines 134-135 to: "This approach results in a small reduction of total burned area, but allows us to produce user friendly global annual layers in both gridded and shapefile format."

The authors conclude that this dataset is useful for emission modelling. In my opinion, the authors should also acknowledge the limitation of this dataset for use in atmospheric models for emission estimates from fires. The Global Fire Atlas does not take into account the smoldering stage of fires, which significantly contribute to gas and particle emissions. In this context, the work of Kaiser et al., 2011 should be mentioned, which uses the fire radiative power for emission estimates. Kaiser, J. W., et al. (2012),

Biomass burning emissions estimated with a global fire assimilation system based on observed fire radiative power, Biogeosciences, 9(1), 527-554, doi:10.5194/bg-9-527-2012.

We fully agree with this suggestion, although our estimates of fire behavior may provide some first guidance on where smoldering may occur (e.g. slow multi-day fires), or where fires may burn more intensely (e.g. high speed), this is further modified by e.g. fuel loads and conditions. Moreover, it often remains unclear how the combination of fire behavior and fuels modify emissions factors (i.e. composition of emissions), and thus eventual emissions of different trace gasses and aerosols.

In the updated manuscript, we will discuss this in more detail. In particular, we will change lines 546-547 to "Large differences in fire behavior across ecosystems and management strategies may improve fire emissions estimates and emissions forecasting, particularly when combined with active fire detections to better characterize different fire stages including the smoldering phase (Kaiser et al., 2012)."

Page 4, line 155: What fraction of local minima is discarded after each iteration step? This information is important for optimization of the number of iteration (which was taken to be 3 in the present work).

During our development phase we had looked into this for a number of individual MODIS tiles, and found that 3 iterations may provide an optimal threshold across different ecosystems. We also found that forest fires may generally require more iterations than fast-moving grassland fires. In the updated manuscript we will include a new supplementary figure visualizing these tradeoffs, to support our decision of 3 iterations (Fig. 1 here).

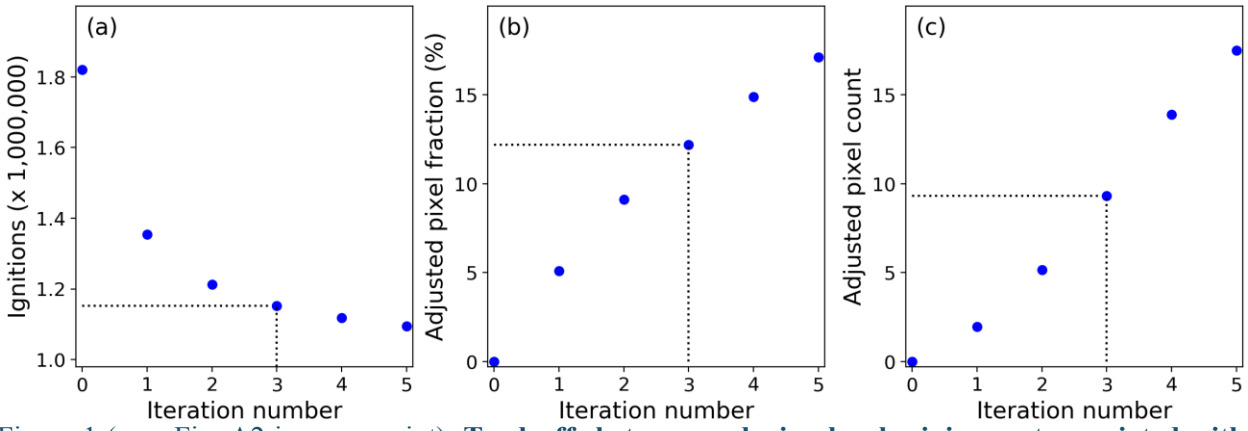

Figure 1 (new Fig. A2 in manuscript): **Tradeoffs between reducing local minima not associated with ignition locations and adjustments made to the global burned area product.** (a) Local minima (ignitions) detected within the daily 500 m global burned area data for 2015 after different number of iterations of the ignition point filter, (b) corresponding fraction of burned area pixels with adjusted burn date, and (c) corresponding number of burned area pixels adjusted divided by the reduction in ignition count. In this study, we used three iterations of the ignition point filter (indicated with the intermittent lines in figures a, b and c), and "0 iterations" refers to the original MCD64A1 col. 6 burned area data.

Figure 4: The horizontal axis legend (burn date (burned area minus active fires)) is not clear to me.

The horizontal axis indicates the difference in burn date between VIIRS active fire detections and the burned area datasets (MCD64A1 c6 and the adjusted burned area data by the Global Fire Atlas). This is calculated as the burn date of the burned area data minus the associated burn date of the (first) corresponding active fire detection. Thus, a negative number indicates that the burned area was detected

before the active fire detection, zero indicates a perfect match, and a positive number indicates that the burned area was detected later than the first active fire detection.

We will change the x-axis label to "Difference in day of burn compared to VIIRS (days)" and change the y-axis label to "Pixel fraction".
Then, we will change the figure caption to: "**Per pixel global comparison of burn dates derived from the MCD64A1 burned area product, adjusted burn dates of the Global Fire Atlas, and VIIRS active fire detections (2012 – 2016).** (a) Forests, (b) shrublands, (c) woody savannas, and (d) savannas and grasslands. Negative values indicate pixels with a burned area day of burn earlier than the first corresponding VIIRS active fire detection, zero indicates no difference in day of burn between both datasets, and positive numbers indicate a delayed detection of burned area compared to active fire detections."

Figure 7: Please check the units in the middle panel (for ignitions).

Although we believe the units are correct, we appreciate that the units on this figure may be somewhat confusing. In particular because we state that burned area is the product of ignitions and size. We think the confusion arises because the exact surface area of a 0.25° grid cell varies with latitude, therefore we feel that for ignitions it makes most sense to report the "ignition density" per unit of area per year. In a similar fashion we report burned area as a fraction per year rather than in square kilometers per year.

For clarity, we will change the figure label "(b) Ignitions (km^{-2} yr^{-1})" to "(b) Ignition density (km^{-2} yr^{-1})". Also, we will further clarify this in the figure caption: "**Figure 8: Average global burned area (MCD64A1), ignition density, and fire size over the study period 2003 – 2016.** For any given area (a) burned area in km^2 per year would be the product of (b) ignitions per year and (c) fire size in km^2. However, because the size of a 0.25° grid cell varies with latitude we have converted the units of burned area to fraction (%) per year and of ignitions to number per km^2 per year for spatial consistency."

The discussion regarding fire direction on page 14 is relatively weak. The fire directions are highly variable depending on topographical features, prevalent wind field and fuel availability. What can one conclude from such variable fire direction and how this information is useful?

We had also anticipated a stronger effect of the dominant wind direction. Therefore, we think that variability in fire direction is an interesting finding on its own. As we show, landscape features and other factors play an important role in fire spread direction, leading to heterogeneous patterns of fire spread in all biomes. This finding may help improve global fire models, for example, since models often assume that fire growth can be described by relatively simple growth equations with homogenous fuel beds. Our work adds to an increasing body of evidence that landscape heterogeneity and associated variability in fuel conditions have a strong influence on global fire behavior across scales.

We will add an additional sentence to the discussion section to highlight to potential new insights for fire modeling (line 546):
"In a similar fashion, many models assume relatively homogeneous fuel beds, while our results suggest that landscape features and vegetation patterns result in highly heterogeneous fuel beds that form a strong control on fire spread (speed and direction)."

The Global Fire Atlas dataset is available for the year 2003-2016. Will this dataset be continuously updated? Given that the dataset is so important, the authors should provide information of update frequency and policy.

We aim to update the dataset annually, with a delay of about 1 year. Because of the "per fire year" processing the algorithm requires burned area data up to 6 months after the calendar year ends to process a given year while the burned area product (MCD64A1 col. 6) is also released with a few months delay.

We will also mention this in the "Data availability" section: "The data are freely available at http://www.globalfiredata.org in standard data product formats and updates for subsequent years will be distributed pending availability of MCD64A1 burned area data and associated research funding."

Reference:

Kaiser, J. W., Heil, A., Andreae, M. O., Benedetti, A., Chubarova, N., Jones, L., Morcrette, J. J., Razinger, M., Schultz, M. G., Suttie, M. and van der Werf, G. R.: Biomass burning emissions estimated with a global fire assimilation system based on observed fire radiative power, Biogeosciences, 9(1), 527–554, doi:10.5194/bg-9-527-2012, 2012.

Reviewer # 2 suggestions and author response

The paper is relevant as it tries to provide a new approach to the analysis of fire regimes, by analyzing different parameters of individual fires extracted from global burned area products. This effort is relevant to better parameterize fire models, as well as to understand fire trends affected by changing climate and socio-economic conditions.

We thank the reviewer for his/her review and thoughtful suggestions. Please find a detailed response to the individual suggestion along with proposed changes below. Note that we will upload the updated manuscript using track change (in response to both reviews) in a separate post.

The main problem I found in this paper is their ambition to qualify single fire activity from a product that was not derived from this purpose. Recent papers (Padilla et al., 2015; Padilla et al., 2014) have found that global burned area products have important omission and commission errors, particularly for small fires Chuvieco et al., 2018; Roteta et al., 2018. They provide a good image of fire activity at global scale, meanwhile the analysis is done at global or at much continental scale. However, establishing characteristics of single fires from these products may be quite misleading. If the authors do not provide better validation datasets, the parameters they analyze at global scale may be in fact confusing. In my view, this is the main weakness of the paper. The authors are assuming estimations from a dataset that is not really validated. Until the MCD64A1 is fully validated, and we better understand their strengths and weaknesses, deriving such detailed analysis as presented in this paper may create more confusion than knowledge.

We appreciate this suggestion, and are aware of the shortcomings of moderate resolution (500-m) satellite imagery (e.g. omission of small fires). Unfortunately, the high resolution satellite data (e.g. Landsat or Sentinel-2) and derived products do not provide the temporal accuracy required to track individual fires and their behavior. In response to this comment, we would like to make the following clarifications. First, the use of moderate resolution satellite imagery to track individual wildfire behavior is an already widely used concept (e.g. Loboda and Csiszar, 2007; Archibald and Roy, 2009; Veraverbeke et al., 2014; Hantson et al., 2015; Benali et al., 2016; Frantz et al., 2016; Fusco et al., 2016; Nogueira et al., 2016; Oom et al., 2016; Laurent et al., 2018). Building on these previous studies, our manuscript provides an improved global approach to identify individual fires and characterize their behavior based on an algorithm that identifies ignition locations and then tracks how the fire expands through time. Second, our aim was to develop a flexible algorithm that leverages availability of daily satellite observations at moderate resolution but can be applied easily to other (global) daily burned area data sets. The MCD64A1 col. 6 burned area product (succeeding MCD45 and MCD64A1 col. 5) is currently among the most widely used and best performing global burned area products (e.g. Padilla et al., 2015; Giglio et al., 2018; Humber et al., 2018), hence our choice for this data set. The MCD64A1 col. 6 data has now been officially released by NASA and was Stage-2 validated against 108 Landsat scenes (Giglio et al., 2018), and although we are looking forward to see additional validation, we see no reason why the data should not be used in the interim. Given the aim of our work (i.e. to develop a flexible algorithm to track individual fire behavior in daily global burned area products), we focus on the quality of the derived products (e.g. burn date accuracy), rather than on absolute burned area (e.g. omission of small fires), although clearly many of these aspects are not entirely independent. During the coming years, we are looking forward continue to develop our algorithm and apply it to the latest generation of improved daily burned area products, e.g. from VIIRS. Moreover, there would be no reason why our algorithm could not be applied to high resolution (20/30m) satellite data, if (close to) a near daily revisiting time would be achieved within the next decade or so.

In response to this suggestion we will include additional validation data (see detailed response below) and we will make several textual clarifications to more extensively discuss previous work, highlight the objectives of our paper, and the dependency of our "derived" product on the underlying burned area data. Specifically, we will make the following textual changes:

Line 107 "The Global Fire Atlas algorithm can be applied to any moderate resolution daily global burned area product, and the quality of the resulting dataset depends both on the Fire Atlas algorithm as well as the underlying burned area estimates. Here we applied the algorithm to the MCD64A1 collection 6 burned area dataset (Giglio et al., 2018) and the minimum detected fire size is therefore one MODIS pixel (21 ha). Several studies have shown that the MCD64A1 col. 6 burned area product provides a considerable improvement compared to previous generation of moderate resolution global burned area products (Padilla et al., 2015; Giglio et al., 2018; Humber et al., 2018)."

Line 552: "The Global Fire Atlas methodology builds on a range of previous studies that have used daily moderate resolution satellite imagery to estimate individual fire sizes (Archibald and Roy, 2009; Hantson et al., 2015; Frantz et al., 2016; Andela et al., 2017), shape (Nogueira et al., 2017; Laurent et al., 2018), duration (Frantz et al., 2016) and spread dynamics (Loboda and Csiszar, 2007; Coen and Schroeder, 2013; Sá et al., 2017)."

Line 568: "In line with previous studies, we found that the coarser resolution (500 m) of the MODIS burned area data used to develop the Global Fire Atlas sometimes underestimated overall burned area (e.g. Randerson et al., 2012; Roteta et al., 2019), fragmenting individual large fires. However, the Landsat-based MTBS data at 30 m resolution were unable to distinguish individual fires within large burn patches of fast-moving grassland fires based on infrequent Landsat satellite overpasses (Fig. B2)."

Line 604: "The Global Fire Atlas algorithm provides a flexible framework that can be easily adjusted to work at different spatial and/or temporal resolutions."

In fact the comparison (validation is not an adequate term for what the authors include in the manuscript) analysis show a high degree of uncertainty even for the simplest variable (fire perimeter). When perimeters are compared with those derived from higher resolution data (MTBS), the correlations are low (for the authors, line 578: they are "reasonable correlations (r2 ranging from 0.3 to 0.5)", but we should remember that they imply than 70-50% of the variance is unexplained). Therefore, in my opinion the subsequent analyses derived from this dataset are quite likely to be erroneous. The comparison they made with active fires and MTBS shows also poor agreements in all biomes. What about fire speed or direction?

I suggest that they at least compare their results with specific very large fires where fire growth is available for different forest services, to check if at least for those large fires their estimations are correct. Very large fires could also be assessed using Landsat data, at least for fire perimeter-size and shape. Are you sure that Australia had a single fire of 42.000 km2? They could also compare their outputs with models of global fire weather conditions (Jolly et al., 2015; Pettinari and Chuvieco, 2017), as well as include some comparisons with fire spread and duration published by fire behavior experts.

The numbers ("r^2 ranging from 0.3 to 0.5") refer to the fire duration estimates that have higher uncertainty than perimeters (read line 578: "Reasonable correlations (r^2 ranging from 0.3 to 0.5) were found between Global Fire Atlas and fire duration estimates .."), that show an average r^2 of 0.51 across land cover types. We appreciate that much of the variance remains unexplained, but we are encouraged by these results. For example, although Landsat-based MTBS provides better estimates of overall burned area, the underlying data lack the temporal revisit frequency to identify individual fires in low biomass ecosystems where fires are typically short and move fast. As we will show in our new supplementary figure (Fig. 1 here), the Global Fire Atlas clearly outperforms MTBS in terms of identifying individual ignition locations, which

explains why the r^2 values of fire perimeters drop from 0.65 in forests to 0.38 for grasslands (a similar decline in agreement was found for fire duration, with r^2=0.51 for forest and r^2=0.33 for grasslands). This is an important finding on its own, since MTBS is a widely used dataset. Because the uncertainty arises both from the Global Fire Atlas and the (combined) MTBS and VIIRS datasets, the use of least square regression is in fact not representative for estimating data quality, we therefore also use orthogonal distance regression that accommodates uncertainties in both datasets and shows better overall agreement.

Although we agree that an extensive comparison to daily fire perimeters would be a great form of validation for day-of-burn, fire duration, expansion rates and final perimeter, these data are unfortunately not available at the ease and scale that the reviewer suggests. In response to this suggestion we have requested available data from the US Forest Service and manually compiled a small dataset consisting of 15 fires that were reasonably well documented (this is not the case for the majority of fires). In line with good agreement between Global Fire Atlas and MTBS estimates of fire perimeters in forested ecosystems (Figs. 5 and 6 in manuscript), very good agreement was found between Global Fire Atlas estimates and US Forest Service estimates of fire size (km^2; r^2=1.00), duration (days; r^2=0.87), and daily expansion ($km2\ day^{-1}$; r^2=0.97; see Fig. 2 here). The comparison also highlights some of the shortcomings of the Global Fire Atlas data that we already discuss; for example, we observed that the Global Fire Atlas tended to somewhat underestimate fire size and overestimate (small) fire duration, resulting in conservative estimates of fire expansion.

These data also allowed us to explore how well the Global Fire Atlas characterizes fire growth dynamics (Fig. 3 here). We find very good agreement between Global Fire Atlas and US Forest Service estimates of fire size at any specific point in time (r^2=1.00), good agreement between a 3-day running average of fire expansion rates from both sources (r^2=0.94), and somewhat reduced agreement for daily expansion rates from both sources (r^2=0.79). This reduced performance for daily estimates originates from the considerable uncertainty in the exact burn date in the burned area product (see Fig. 4 in manuscript), and thus the attribution of fire expansion rates to a specific day. In addition, we find that the Global Fire Atlas data compares particularly well for large fires or expansion rates, with lower r^2 values for smaller fires and expansion rates (e.g. compare upper and lower panels of Figs. 2 and 3 here). The combination of very precise fire perimeter maps from the US Forest Service and the focus on large fires, likely explains why the Global Fire Atlas shows better agreement in Fig. 2 here compared to Fig. 5 in the manuscript. Therefore we expect that extremely large fires, like the fire in Australia the reviewer mentions, are among the fires that are best captured by the Global Fire Atlas data. Large fires are generally well mapped by moderate resolution burned area algorithms (e.g. Fusco et al., 2019) as well as easy to characterize from the Global Fire Atlas perspective.

To respond to the specific comment concerning the suggestion of comparing our estimated daily fire behavior to fire weather indices, we have great interest in this, and it is something we are currently working on in a separate manuscript.

In addition to the new figures (Fig. 1-3 here), we will make a number of textual additions/clarifications:

Line 276: “Finally, we compared Global Fire Atlas data to a small (manually compiled) dataset of daily fire perimeters from the US Forest Service.”

Line 318: “For specific large wildfires across the western USA, the US Forest Service National Infrared Operations (NIROPS; https://fsapps.nwcg.gov/nirops/) derives estimates of daily fire perimeters for fire management purposes by collecting night-time high resolution infrared imagery. This imagery is manually analyzed by trained specialists to extract the active fire front. Although these data provide a wealth of information, only few fires were completely and precisely documented. From their database we were able to extract 15 large fires for which daily perimeter information was available. Although

insufficient for full scale validation, results provide valuable insights into the strengths and shortcomings of the Global Fire Atlas estimates of individual fire size, duration and expansion rates. In addition, we compared day-to-day expansion rates (km^2 day^{-1}) of individual large fires across both datasets. If multiple Global Fire Atlas perimeters overlapped with a single US Forest Service fire perimeter, we compared the fires with the largest overlapping surface area."

Line 346: "In line with these findings, we found good agreement between a 3-day running average of Global Fire Atlas and US Forest service estimates of daily fire expansion, but reduced correspondence for daily estimates of fire growth rates due to uncertainty in the day-of-burn of the burned area product (Fig. B1)."

Line 392: "The comparison of Global Fire Atlas data to a small dataset (n = 15) of daily perimeters of large wildfires in primarily forested cover types mapped by the US Forest Service yielded good correspondence between estimates of fire size, duration, and expansion rates (Fig. 7). The improved comparison of fire size (cf. Fig. 5a and 7a) could be related to the US Forest Service data being more accurate than MTBS, but likely also represents the good performance of the Global Fire Atlas (e.g. compare Figs. 7a, b and c to Figs. 7d, e and f) and underlying burned area products (Fusco et al., 2019) for relatively large fires. In contrast to the suggested underestimate of fire duration shown in Fig. 6a, these data suggest the Global Fire Atlas may slightly overestimate fire duration. This difference may reflect the fact that active fire detections may be triggered by smoldering while the burned area product will only register the initial changes in surface reflectance from fire. Based on a small underestimate of overall burned area and overestimate of fire duration by the Global Fire Atlas, the average daily fire expansion rates based on US Forest Service data were higher than estimates based on Global Fire Atlas data (Fig. 7c and f)."

Line 583: "Moreover, the uncertainty in the burn date of the underlying burned area product is typically at least one day, resulting in a large uncertainty in the fire duration estimates of shorter fires. Global Fire Atlas data therefore performed best for large fires (Figs. 6 and 7)."

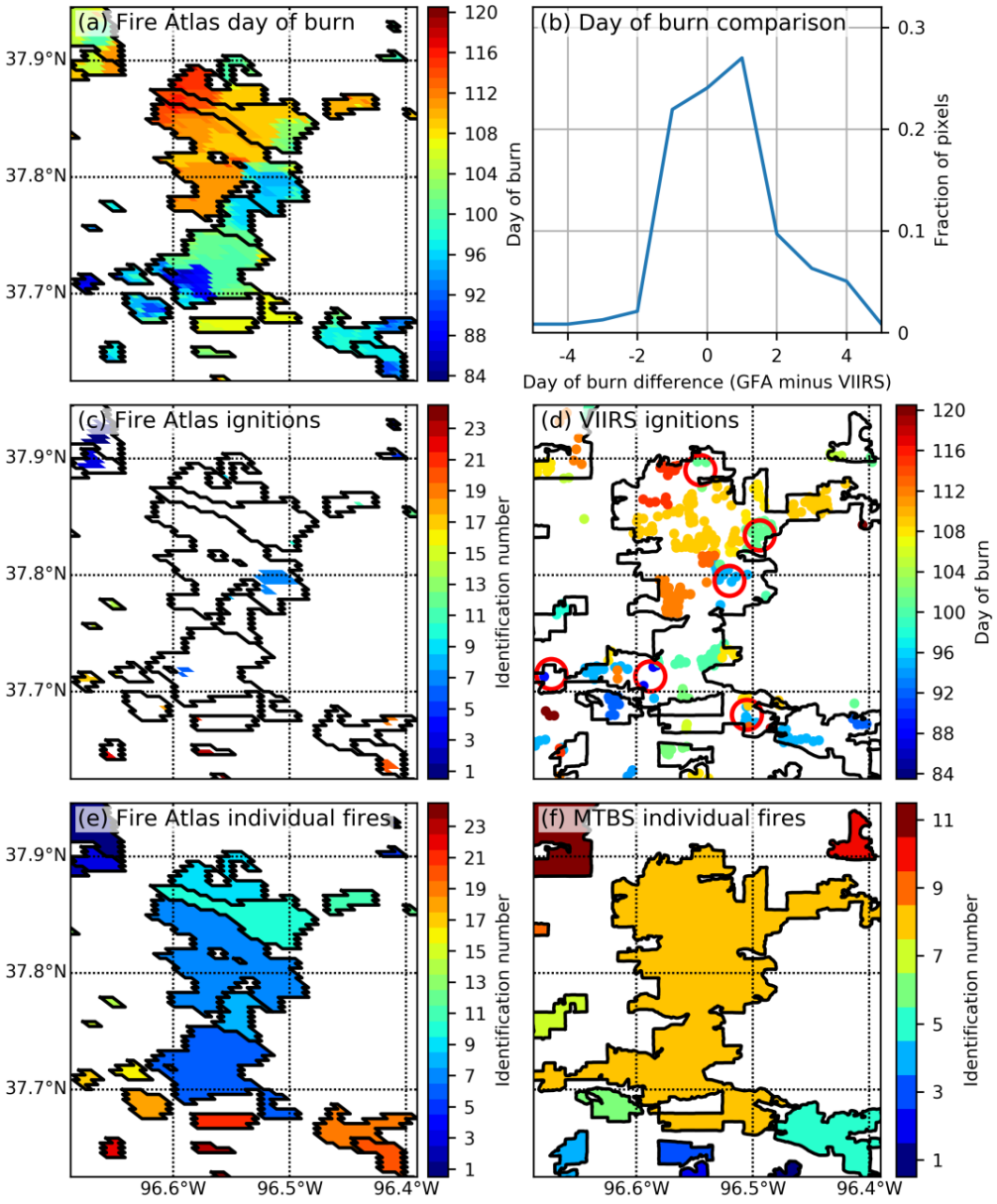

Figure 1 (Fig. B2 in updated manuscript): **Comparison of Global Fire Atlas perimeters and ignition locations to estimates based on MTBS and VIIRS for frequently-burning grasslands in Kansas, USA.** (a) Global Fire Atlas adjusted burn dates from MCD64A1, (b) per-pixel comparison of adjusted burn dates used within the Global Fire Atlas (GFA) to the day of the (first) active fire detection from VIIRS, (c) ignition points as estimated by the Global Fire Atlas, (d) manually interpreted ignition locations (red circles) based on VIIRS active fire detections on top of MTBS fire perimeters, (e) individual fires as estimated by the Global Fire Atlas, and (f) the MTBS burned area and individual fires. Here, MCD64A1 data underestimates the total burned area compared to the visual interpretation of Landsat data within the MTBS project, resulting in fragmentation of individual large fires. However, the daily temporal resolution of MODIS imagery allows the Global Fire Atlas to distinguish individual fires and ignition points within larger burn scars that cannot be resolved from infrequent Landsat observations used to delineate fire perimeters within the MTBS project. Broad patterns of ignition locations identified by the Global Fire Atlas are confirmed by manual interpretation of patterns inferred from VIIRS active fire detections (d).

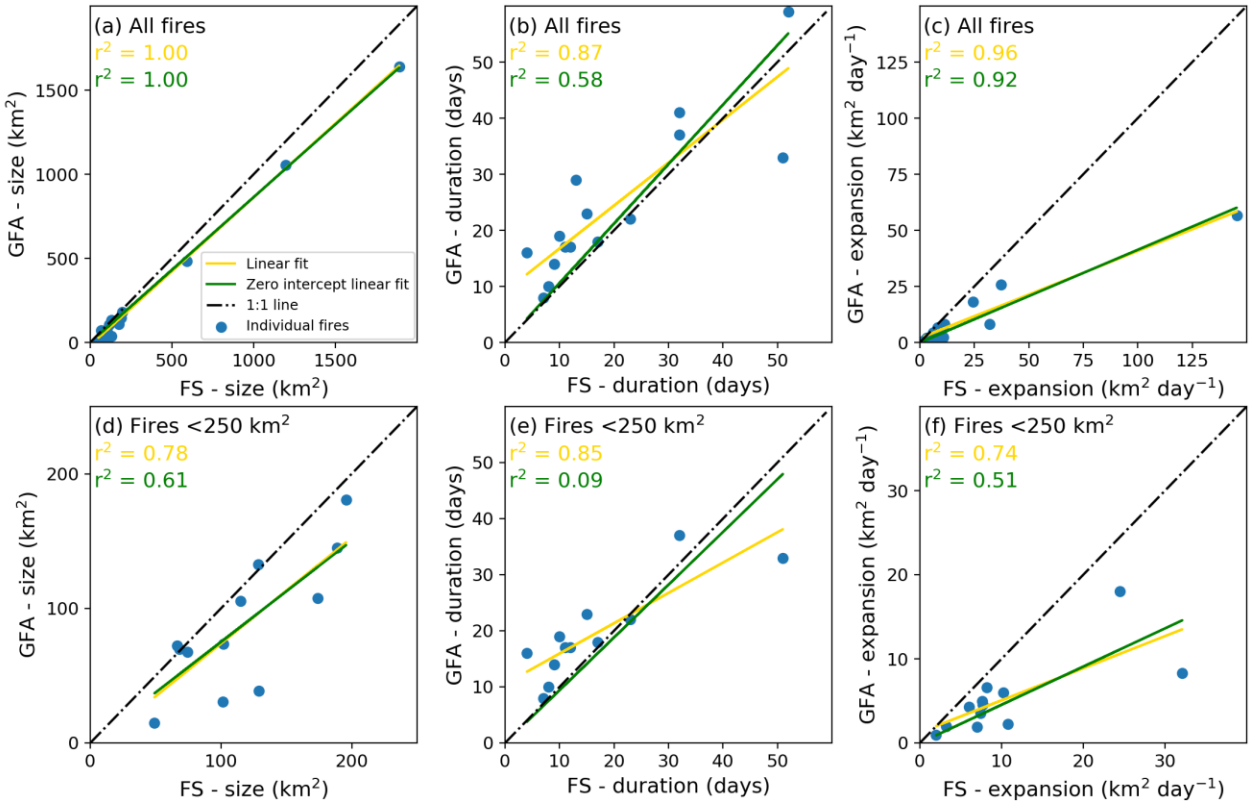

Figure 2 (new Fig. 7): **Comparison of Global Fire Atlas (GFA) and US Forest Service (FS) data for a selected number of large wildfires in the US.** Comparison of (a) fire size, (b) duration, and (c) average daily expansion rate for all fires (N=15), (d, e and f) are like (a, b and c) but for fires smaller than 250 km^2 (N=12). Correlation coefficients are provided based on linear regression with (yellow) and without (green) intercept, assuming a non-zero intercept could indicate a structural offset between both datasets.

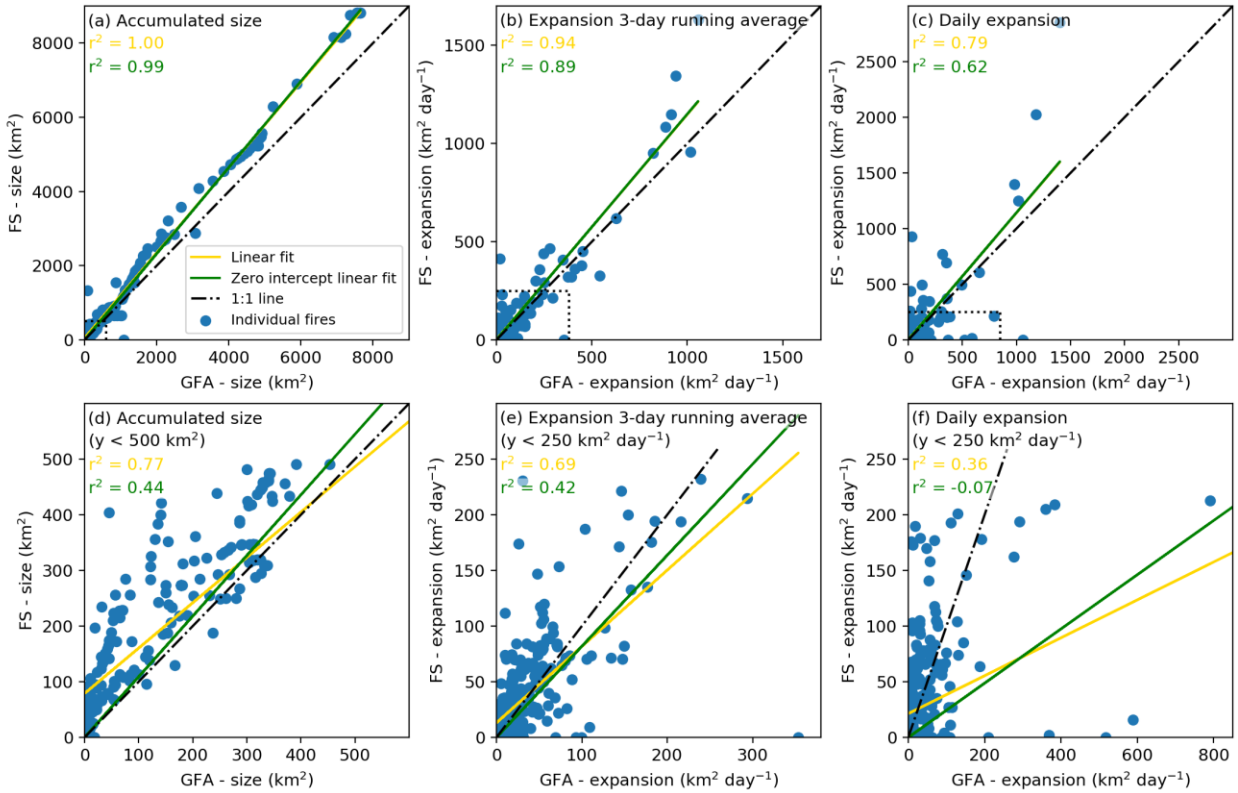

Figure 3 (new **Figure B1): Comparison of daily Global Fire Atlas and US Forest Service data for a selected number of well characterized wildfires in the US.** (a) The accumulated daily fire size (for all fires, N=15) illustrates the ability of the Global Fire Atlas to reproduce individual large fire sizes at any specific day over the fire lifetime (each blue dot indicates the size of a specific fire on a specific day). (b) A 3-day running average of the daily growth or "expansion" of each fire (km^2 day^{-1}) and (c) the daily expansion on each day of each fire. Figures (d), (e), and (f) are like (a), (b), and (c), but for US Forest Service fire sizes smaller than 500 km^2 or expansion rates lower than 250 km^2 day^{-1} and corresponding Global Fire Atlas estimates (see intermittent boxes on top-figures).

On the other hand, I doubt about the utility of providing global averages of different fire parameters, such as fire duration or progression by continent. In this regard, some of the comments included in the results section may seem quite trivial or difficult to justify empirically. What is the point of concluding that "fire duration exerted a strong control on fire size and total burned area"? Is this not the case in the vast majority of fires?

Although this may seem trivial, the vast majority of fire models currently do not include multi-day fires (e.g. Hantson et al., 2016; Rabin et al., 2017). Our study now for the first time shows that multi-day fires are the norm across all ecosystems and in some ecosystems "duration" exerts a strong control on eventual fire size and total burned area while fire speed is more important in other ecosystems. Incorporating these mechanisms into fire-enabled global ecosystem models is thus critical to capture the (changing) role of fire in the Earth system. We think it is exciting that with these new data we are now for the first time able to analyze how fire behavior influences fire size distributions and eventual burned area. We believe that summarizing these data across continental or ecosystem scales provides a good lookup table for e.g. fire modelers to see whether their model results are within the right range.

In summary, the authors should make an additional effort to really validate their product and better identify the weaknesses of current analysis.

We very much appreciate the suggestion of the reviewer that additional validation data would be helpful, but these data are unfortunately not as readily accessible as the reviewer suggests. In response to this suggestion we have manually compiled a small dataset of well characterized daily behavior of forest fires in the US. Results clearly demonstrate the ability of the Global Fire Atlas to assess individual fire behavior but also illustrate some of the specific shortcomings that we now discuss in more detail. During the coming years we are very much looking forward to further develop our data product as well as provide improved validation and optimization of parameters based on new data availability.

Specific comments

Line 45: Worldwide, fires burn an area larger than the size of the European Union every year (Randerson et al.,2012; Giglio et al., 2013). Please include total area in km2, the reader does not need to know the size of the European union to understand your sentence.

We believe the reader will understand this sentence without knowing the exact size of the European Union as we simply mean "a large area".

Line 55: you claim that burned area reduction is occurring in the last two decades, but Andela et al., 2017 paper refers only to the 2001-2017 period (1995-2001 with more uncertainty), so you could only claim that the reduction is observed in the last few years, as you do not have date from several decades ago.

The study of Andela et al. (2017) included 18 years of data, we will change "Over the past two decades, .." to "Over the past 18 years, .."

Line 65: Our understanding of global fire activity is also severely constrained by the coarse resolution data we are based on our analysis. Recent analysis of burned area estimation comparing coarse and medium resolution data shows that in fact we may be losing a significant part of fire activity (Roteta et al., 2018, https://geogra.uah.es/fire_cci/sfd.php), particularly in tropical regions.

We appreciate the importance of small fires (e.g. Randerson et al., 2012), and we will more clearly discuss the advantages and limitations of the different datasets in our manuscript (see also updated Fig. B2 (Fig. 1 here) and corresponding discussion above). However, we would like to keep our introduction focused on characterizing global fire behavior instead of other important issues that we do not contribute to in this work.

Specifically, we will update line 568: "In line with previous studies, we found that the coarser resolution (500 m) of the MODIS burned area data used to develop the Global Fire Atlas sometimes underestimated overall burned area (e.g. Randerson et al., 2012; Roteta et al., 2019), fragmenting individual large fires. However, the Landsat-based MTBS data at 30 m resolution were unable to distinguish individual fires within large burn patches of fast-moving grassland fires based on infrequent Landsat satellite overpasses (Fig. B2)."

Line 88: update (Giglio et al., submitted)

Done

Lines 155-164: How did you proceed in the case of small fires (a few pixels)? You claim that local minima are deleted when they do not spread forward in time.

In case there is no "later burn date", the ignition point(s) associated with the largest possible number of iterations were retained. We will clarify this in the text.

Line 160: "For short duration fires, the ignition points were retained associated with largest possible number of iterations."

Lines 180-187: Fire spread is obviously associated to wind speed and slope, not just to fuel availability. Therefore the assumptions made by the authors seem quite arbitrary for a global product. Have they made any validation of their persistence algorithm? It is not clear what happened with areas that burned 2 times, were they assigned 6 or 8 day persistency? The thresholds are in fact overlapped.

Our "fire persistence threshold" is somewhat similar to the "cut off" value previously used in flood fill based approaches (e.g. Archibald and Roy, 2009; Hantson et al., 2015; Nogueira et al., 2016; Oom et al., 2016; Laurent et al., 2018). However, in contrast to the flood fill based algorithms, we force the fires to only move forward in time (i.e. logical progression), which can be done because we first apply the ignition point filter that removes small inconsistencies in the burn date estimates. Our threshold values (i.e. 4, 6, 8, or 10 days) were mostly based on the idea that if fire frequencies are low, the probability of multiple fires occurring in each other's vicinity is likely low, hence we can use a longer threshold. In areas of frequent (human caused) fires on the other hand, it is not unlikely to have a new ignition point in the vicinity of a burn scar from a previous fire, in this case we use a short threshold to reduce the likelihood of independent fires to be merged artificially. Fire frequency is also closely related to vegetation patterns, hence we notice that our thresholds are broadly biome dependent (e.g. typically 10-day thresholds in high fuel load boreal and temperate zones and low 4-day thresholds in frequently burning savannas and grasslands).

Following the reviewer's suggestion, we propose to make the following textual clarifications:

Line 185: We will change line 185 to ".., and a 6, 8 and 10-day fire persistence period for grid cells that burned 3 times, 2 times, or 1 time, respectively." to be more precise.

Line 560: "Interestingly, we found similar spatial patterns of fire size (cf. Fig. 8 and Archibald et al., 2013; Hantson et al., 2015), although absolute estimates may show large differences based on the "cut off" value used within the flood-fill approach (Oom et al., 2016), and to a lesser extent by the fire persistence threshold used here."

Line 195. It is not clear if two active fires that merged were assigned a single perimeter or two. It seems they were divided, but most forest services would probably consider them as single one.

We define a single fire as having one ignition point, so several fires that merge would be considered independent fire events in our dataset. This is indeed one of the reasons that our data deviate from the MTBS (also see our response to your earlier suggestions). This is explained in more detail in section 2.1.

Lines 240-: : : It is not clear what the authors did when areas were not observed by clouds or cloud shadows. What is the impact of unobserved periods in fire progression? Were the geometrical deformation effects caused by off-nadir observations taken into account?

We use the MCD64A1 burned area product without any further modification, therefore the uncertainty in the day-of-burn would likely increase during periods of cloud cover (we also mention this, e.g. lines 171-173). Similarly, the scan angle of MODIS instruments (or data-gaps) could potentially affect the correct attribution of burned area to a given day. In fact, this is the reason we let our time series start in 2003, when the combination of the MODIS instruments aboard both Terra and Aqua provide more frequent

observations (see lines 89-90). Nevertheless, the uncertainty in burn date will affect Global Fire Atlas fire characterization, in particular of small and short fires. For example, a multi-pixel single day fire could easily get a longer fire duration assigned solely based on the uncertainty of the burn date in the burned area product. For large multi-day fires, these effects become smaller (e.g. Figs. 4 and 6 of manuscript). Based on the additional comparison of the Global Fire Atlas and US Forest Service data we will more clearly discuss the consequences of uncertainties in the burn date:

Line 340 "Several factors may account for the positive bias in the 500 m day of burn from burned area compared to active fire detections, including orbital coverage, cloud and smoke obscuration, and different thresholds between burned area and active fire algorithms regarding the burnt fraction of a 500 m grid cell."

Line 346 "). In line with these findings, we found good agreement between a 3-day running average of Global Fire Atlas and US Forest service estimates of daily fire expansion, but reduced correspondence for daily estimates of fire growth rates due to uncertainty in the day-of-burn of the burned area product (Fig. B1)."

Figure 3 shows direction of spread that are not very realistic, as all sort of directions are included, even for neighbor pixels (North and South directions in contiguous areas??)

The reviewer should remember that a single pixel represents 21 ha, and may contain numerous landscape features that form natural barriers to fire and could change the fire direction (e.g. vegetation patterns, gullies etc.). Nevertheless, it is true that on a per-pixel level the direction estimate may be quite uncertain, this figure mostly serves to demonstrate how the algorithm works (i.e., for each pixel between fire lines it is estimated how the fire has moved, which results in a speed and direction of spread). Because of the uncertainty at the individual pixel level (e.g. see Fig. 4), we report dominant direction including only multi-day fires larger than 10 km^2 in our global map (Fig. 9).

It is not clear why did you include MCD64 in Figure 4, as the date information should be the almost the same as the Global Fire Atlas. I would recommend changing it to a single graph showing dating accuracy for the four major biomes.

We include the MCD64A1 col. 6 data to demonstrate that despite the filters we apply, the overall adjustment of the burn date by the Global Fire Atlas algorithm was small.

Lines 343-346: "The adjustments made to the burn date here, required to effectively determine the extent and duration of individual fires, had a relatively small effect on the overall accuracy but tended to reduce the negative bias in burn dates and increase the positive bias (i.e. delayed burn date compared to active fire detection, see red and black lines in Fig 4)."

The fire dominant direction will probably be more useful for fire modelers expressed in degrees.

Converting the dominant direction to degrees can be achieved by multiplying the numerical dominant direction (ranging from 0-8) by 45. We will include this suggestion in the online user guide.

Other authors have done similar analysis, a recent one by Laurent et al., 2018. Line 440. I doubt that any fire behavior modeler would agree with: "the dominant direction typically represented less than half of the pixels". I think the approach by Laurent et al (2018) using the dominant direction of the evolving ellipsis is more adequate in this regard, as most fires have a dominant wind direction.

We appreciate that fire direction may be estimated in various ways, with likely similar outcomes. We have chosen for the approach we present in our manuscript because it is "internally consistent", in other words, fire direction and speed are derived at the same time when we calculate the most logical (i.e. shortest distance) path the fire may have followed. The exciting thing about the Global Fire Atlas and similar datasets is that, based on the characterization of about one million individual fires worldwide each year, we can now actually investigate what "most" fires do. Our first results indicate that, although dominant wind direction was important, landscape features may be more important than previously thought.

I do not understand the meaning of using average NDVI values to show extreme fires. I do not see the relation.

The NDVI map on the background provides the reader an idea of vegetation cover and available fuels, closely related to fire occurrence and behavior (e.g. Bowman et al., 2009).

We have now clarified this "The background image depicts mean MODIS normalized difference vegetation index (NDVI, 2003 – 2016), an indicator for large scale vegetation patterns and available fuels."

References

Chuvieco, E., Lizundia-Loiola, J., Pettinari, M. L., Ramo, R., Padilla, M., Tansey, K., Mouillot, F., Laurent, P., Storm, T., Heil, A., and Plummer, S.: Generation and analysis of a new global burned area product based on MODIS 250 m reflectance bands and thermal anomalies, Earth Systems Science Data, 2018, 2015-2031, Doi: https://doi.org/10.5194/essd-10-2015-2018, 2018.

Jolly, W. M., Cochrane, M. A., Freeborn, P. H., Holden, Z. A., Brown, T. J., Williamson, G. J., and Bowman, D. M.: Climate induced variations in global wildfire danger from 1979 to 2013, Nature Communications, 6, Doi: 10.1038/ncomms8537, 2015.

Laurent, P., Mouillot, F., Yue, C., Ciais, P., Moreno, M. V., and Nogueira, J. M. P.: FRY, a global database of fire patch functional traits derived from space-borne burned area products, Scientific Data, 5, 180132, Doi: 10.1038/sdata.2018.132, 2018.

Padilla, M., Stehman, S. V., and Chuvieco, E.: Validation of the 2008 MODIS-MCD45 global burned area product using stratified random sampling, RSE, 144, 187-196, Doi: http://dx.doi.org/10.1016/j.rse.2014.01.008, 2014.

Padilla, M., Stehman, S. V., Hantson, S., Oliva, P., Alonso-Canas, I., Bradley, A., Tansey, K., Mota, B., Pereira, J. M., and Chuvieco, E.: Comparing the Accuracies of Remote Sensing Global Burned Area Products using Stratified Random Sampling and Estimation, RSE, 160, 114-121, Doi: http://dx.doi.org/10.1016/j.rse.2014.01.008, 2015.

Pettinari, M., and Chuvieco, E.: Fire Behavior Simulation from Global Fuel and Climatic Information, Forests, 8, 179, 2017. Roteta, E., Bastarrika, A., Storm, T., and Chuvieco, E.: Development of a Sentinel-2 burned area algorithm: generation of a small fire database for northern hemisphere tropical Africa RSE, (in review), 2018.

References

Andela, N., Morton, D. C., Giglio, L., Chen, Y., Van Der Werf, G. R., Kasibhatla, P. S., Defries, R. S., Collatz, G. J., Hantson, S., Kloster, S., Bachelet, D., Forrest, M., Lasslop, G., Li, F., Mangeon, S., Melton, J. R., Yue, C. and Randerson, J. T.: A human-driven decline in global burned area, Science, 356,

1356–1362, doi:10.1126/science.aal4108, 2017.

Archibald, S., Lehmann, C. E. R., Gómez-Dans, J. L. and Bradstock, R. A.: Defining pyromes and global syndromes of fire regimes, Proc. Natl. Acad. Sci. U. S. A., 110, 6442–6447, doi:10.1073/pnas.1211466110, 2013.

Archibald, S. and Roy, D. P.: Identifying individual fires from satellite-derived burned area data, IEEE Int. Geosci. Remote Sens. Symp. Proc., 9, 160–163, doi:10.1109/IGARSS.2009.5417974, 2009.

Benali, A., Russo, A., Sá, A. C. L., Pinto, R. M. S., Price, O., Koutsias, N. and Pereira, J. M. C.: Determining fire dates and locating ignition points with satellite data, Remote Sens., 8, 326, doi:10.3390/rs8040326, 2016.

Bowman, D. M. J. S., Balch, J. K., Artaxo, P., Bond, W. J., Carlson, J. M., Cochrane, M. A., D'Antonio, C. M., Defries, R. S., Doyle, J. C., Harrison, S. P., Johnston, F. H., Keeley, J. E., Krawchuk, M. A., Kull, C. A., Marston, J. B., Moritz, M. A., Prentice, I. C., Roos, C. I., Scott, A. C., Swetnam, T. W., van der Werf, G. R. and Pyne, S. J.: Fire in the Earth system, Science, 324, 481–484, doi:10.1126/science.1163886, 2009.

Coen, J. L. and Schroeder, W.: Use of spatially refined satellite remote sensing fire detection data to initialize and evaluate coupled weather-wildfire growth model simulations, Geophys. Res. Lett., 40, 5536–5541, doi:10.1002/2013GL057868, 2013.

Frantz, D., Stellmes, M., Röder, A. and Hill, J.: Fire spread from MODIS burned area data: Obtaining fire dynamics information for every single fire, Int. J. Wildl. Fire, 25, 1228–1237, doi:10.1071/WF16003, 2016.

Fusco, E. J., Abatzoglou, J. T., Balch, J. K., Finn, J. T. and Bradley, B. A.: Quantifying the human influence on fire ignition across the western USA, Ecol. Appl., 26, 2388–2399, doi:10.1002/eap.1395, 2016.

Fusco, E. J., Finn, J. T., Abatzoglou, J. T., Balch, J. K., Dadashi, S. and Bradley, B. A.: Detection rates and biases of fire observations from MODIS and agency reports in the conterminous United States, Remote Sens. Environ., 220, 30–40, doi:10.1016/j.rse.2018.10.028, 2019.

Giglio, L., Boschetti, L., Roy, D. P., Humber, M. L. and Justice, C. O.: The Collection 6 MODIS burned area mapping algorithm and product, Remote Sens. Environ., 217(July), 72–85, doi:10.1016/j.rse.2018.08.005, 2018.

Hantson, S., Arneth, A., Harrison, S. P., Kelley, D. I., Prentice, I. C., Rabin, S. S., Archibald, S., Mouillot, F., Arnold, S. R., Artaxo, P., Bachelet, D., Ciais, P., Forrest, M., Friedlingstein, P., Hickler, T., Kaplan, J. O., Kloster, S., Knorr, W., Lasslop, G., Li, F., Mangeon, S., Melton, J. R., Meyn, A., Sitch, S., Spessa, A., van der Werf, G. R., Voulgarakis, A. and Yue, C.: The status and challenge of global fire modelling, Biogeosciences, 13, 3359–3375, doi:10.5194/bg-2016-17, 2016.

Hantson, S., Pueyo, S. and Chuvieco, E.: Global fire size distribution is driven by human impact and climate, Glob. Ecol. Biogeogr., 24, 77–86, doi:10.1111/geb.12246, 2015.

Humber, M. L., Boschetti, L., Giglio, L. and Justice, C. O.: Spatial and temporal intercomparison of four global burned area products, Int. J. Digit. Earth, 8947, 1–25, doi:10.1080/17538947.2018.1433727, 2018.

Laurent, P., Mouillot, F., Yue, C., Ciais, P., Moreno, M. V. and Nogueira, J. M. P.: FRY, a global database of fire patch functional traits derived from space-borne burned area products, Sci. Data, 5, 180132, doi:10.1038/sdata.2018.132, 2018.

Loboda, T. V. and Csiszar, I. A.: Reconstruction of fire spread within wildland fire events in Northern Eurasia from the MODIS active fire product, Glob. Planet. Change, 56, 258–273, doi:10.1016/j.gloplacha.2006.07.015, 2007.

Nogueira, J. M. P., Ruffault, J., Chuvieco, E. and Mouillot, F.: Can we go beyond burned area in the assessment of global remote sensing products with fire patch metrics?, Remote Sens., 9, 7, doi:10.3390/rs9010007, 2017.

Nogueira, J. M. P., Ruffault, J., Chuvieco, E., Mouillot, F., Frantz, D., Stellmes, M., Röder, A., Hill, J., Veraverbeke, S., Sedano, F., Hook, S. J., Randerson, J. T., Jin, Y., Rogers, B. M., Oom, D., Silva, P. C., Bistinas, I., Pereira, J. M. C., Hantson, S., Pueyo, S., Chuvieco, E., Archibald, S. and Roy, D. P.: Identifying individual fires from satellite-derived burned area data, Remote Sens., 9(1), 160–163, doi:10.1109/IGARSS.2009.5417974, 2016.

Oom, D., Silva, P. C., Bistinas, I. and Pereira, J. M. C.: Highlighting biome-specific sensitivity of fire size distributions to time-gap parameter using a new algorithm for fire event individuation, Remote Sens., 8, 663, doi:10.3390/rs8080663, 2016.

Padilla, M., Stehman, S. V., Ramo, R., Corti, D., Hantson, S., Oliva, P., Alonso-Canas, I., Bradley, A. V., Tansey, K., Mota, B., Pereira, J. M. and Chuvieco, E.: Comparing the accuracies of remote sensing global burned area products using stratified random sampling and estimation, Remote Sens. Environ., 160, 114–121, doi:10.1016/j.rse.2015.01.005, 2015.

Rabin, S. S., Melton, J. R., Lasslop, G., Bachelet, D., Forrest, M., Hantson, S., Kaplan, J. O., Li, F., Mangeon, S., Ward, D. S., Yue, C., Arora, V. K., Hickler, T., Kloster, S., Knorr, W., Nieradzik, L., Spessa, A., Folberth, G. A., Sheehan, T., Voulgarakis, A., Kelley, D. I., Colin Prentice, I., Sitch, S., Harrison, S. and Arneth, A.: The Fire Modeling Intercomparison Project (FireMIP), phase 1: Experimental and analytical protocols with detailed model descriptions, Geosci. Model Dev., 10, 1175–1197, doi:10.5194/gmd-10-1175-2017, 2017.

Randerson, J. T., Chen, Y., van der Werf, G. R., Rogers, B. M. and Morton, D. C.: Global burned area and biomass burning emissions from small fires, J. Geophys. Res., 117, G04012, doi:10.1029/2012JG002128, 2012.

Roteta, E., Bastarrika, A., Padilla, M., Storm, T. and Chuvieco, E.: Development of a Sentinel-2 burned area algorithm: Generation of a small fire database for sub-Saharan Africa, Remote Sens. Environ., 222(September 2017), 1–17, doi:10.1016/j.rse.2018.12.011, 2019.

Sá, A. C. L., Benali, A., Fernandes, P. M., Pinto, R. M. S., Trigo, R. M., Salis, M., Russo, A., Jerez, S., Soares, P. M. M., Schroeder, W. and Pereira, J. M. C.: Evaluating fire growth simulations using satellite active fire data, Remote Sens. Environ., 190, 302–317, doi:10.1016/j.rse.2016.12.023, 2017.

Veraverbeke, S., Sedano, F., Hook, S. J., Randerson, J. T., Jin, Y. and Rogers, B. M.: Mapping the daily progression of large wildland fires using MODIS active fire data, Int. J. Wildl. Fire, 23, 655–667, doi:10.1071/WF13015, 2014.

The Global Fire Atlas of individual fire size, duration, speed, and direction

Niels Andela[1,2], Douglas C. Morton[1], Louis Giglio[3], Ronan Paugam[4], Yang Chen[2], Stijn Hantson[2], Guido R. van der Werf[5], and James T. Randerson[2]

[1]Biospheric Sciences Laboratory, NASA Goddard Space Flight Center, Greenbelt, MD 20771, USA
[2]Department of Earth System Science, University of California, Irvine, CA 92697, USA
[3]Department of Geographical Sciences, University of Maryland, College Park, MD 20742, USA
[4]Centre Europe´en de Recherche et de Formation Avance´e en Calcul Scientifique, URA1875, CNRS, Toulouse, France.
[5]Faculty of Science, Vrije Universiteit Amsterdam, Amsterdam, Netherlands

Correspondence to: Niels Andela (niels.andela@nasa.gov)

Abstract. Natural and human-ignited fires affect all major biomes, altering ecosystem structure, biogeochemical cycles, and atmospheric composition. Satellite observations provide global data on spatiotemporal patterns of biomass burning and evidence for rapid changes in global fire activity in response to land management and climate. Satellite imagery also provides detailed information on the daily or sub-daily position of fires that can be used to understand the dynamics of individual fires. The Global Fire Atlas is a new global dataset that tracks the dynamics of individual fires to determine the timing and location of ignitions and fire size, duration, daily expansion, fire line length, speed, and direction of spread. Here we present the underlying methodology and Global Fire Atlas results for 2003-2016 derived from daily moderate resolution (500 m) Collection 6 MCD64A1 burned area data. The algorithm identified 13.3 million individual fires over the study period, and estimated fire perimeters were in good agreement with independent data for the continental United States. A small number of large fires dominated sparsely populated arid and boreal ecosystems, while burned area in agricultural and other human-dominated landscapes was driven by high ignition densities that resulted in numerous smaller fires. Long-duration fires in the boreal regions and natural landscapes in the humid tropics suggest that fire-season length exerts a strong control on fire size and total burned area in these areas. In arid ecosystems with low fuel densities, high fire spread rates resulted in large, short-duration fires that quickly consumed available fuels. Importantly, multi-day fires contributed the majority of burned area in all biomass burning regions. A first analysis of the largest, longest, and fastest fires that occurred around the world revealed coherent regional patterns of extreme fires driven by large-scale climate forcing. Global Fire Atlas data are publicly available through www.globalfiredata.org, and individual fire information and summary data products provide new information for benchmarking fire models within ecosystem and Earth system models, understanding vegetation-fire feedbacks, improving global emissions estimates, and characterizing the changing role of fire in the Earth system.

1 Introduction

Worldwide, fires burn an area larger than the size of the European Union every year (Randerson et al., 2012; Giglio et al., 2013). The majority of burned area occurs in grasslands and savannas, fire-adapted ecosystems where fires maintain open landscapes by reducing shrub and tree cover (Scholes and Archer, 1997; Abreu et al., 2017). However, all major biomes burn. Climate controls global patterns of fire activity by driving vegetation productivity and fuel build up as well as fuel conditions (Bowman et al., 2009). Humans are the dominant source of ignitions in most flammable ecosystems, but human activities also reduce fire sizes through landscape fragmentation and fire suppression (Archibald et al., 2012; Taylor et al., 2016; Balch et al., 2017).

Over the past ~~two decades~~18 years, socio-economic development and corresponding changes in human land use have considerably reduced fire activity in fire-dependent grasslands and savannas worldwide (Andela et al., 2017). At the same time, warming climate has dried fuels and has increased the length of fire seasons across the globe (Jolly et al., 2015), which is particularly important in forested ecosystems with abundant fuels (e.g., Kasischke and Turetsky, 2006; Aragão et al., 2018). Fire activity increases non-linearly in response to drought conditions in populated areas of the humid tropics (Alencar et al., 2011; Field et al., 2016), resulting in large scale degradation of tropical ecosystems (van der Werf et al., 2008; Morton et al., 2013b; Brando et al., 2014), and extensive periods of poor air quality (Johnston et al., 2012; Lelieveld et al., 2015; Koplitz et al., 2016). Moreover, increasing population densities in highly flammable biomes also amplify the socio-economic impacts of wildfires related to air quality or damage to houses and infrastructure (Moritz et al., 2014; Knorr et al., 2016). Despite the importance of understanding changing global fire regimes for ecosystem services, human well being, climate, and conservation, our current understanding of changing global fire regimes is limited because existing satellite data products detect actively burning pixels or burned area, but not individual fires and their behavior.

Frequent observations from moderate-resolution, polar-orbiting satellites may provide information on individual fire behavior in addition to estimates of total burned area. Several recent studies have shown that fire-affected pixels can be separated into clusters based on spatial and temporal proximity. This information can be used to study the number and size distributions of individual fires (Archibald and Roy, 2009; Hantson et al., 2015; Oom et al., 2016), fire shapes (Nogueira et al., 2017; Laurent et al., 2018), and the location of ignition points (Benali et al., 2016; Fusco et al., 2016). One limitation of fire clustering algorithms that rely on spatial and temporal proximity of fire pixels is the inability to separate individual fires within large burn patches that contain multiple ignition points, a frequent phenomenon in grassland biomes. To address the possibility of multiple ignition points, other algorithms have specifically tracked the spread of individual fires in time and space, with demonstrated improvements for isolating ignition points and constraining final fire perimeters (Frantz et al., 2016; Andela et al., 2017). In addition to the size and ignition points of individual fires, other studies used daily or sub-daily detections of fire activity to track growth dynamics of fires (Loboda and Csiszar, 2007; Coen and Schroeder, 2013; Veraverbeke et al., 2014; Sá et al., 2017). Together, these studies highlight the strengths and limitations of using daily or sub-daily satellite imagery to derive information on individual fires and their behavior over time.

Here we present the Global Fire Atlas of individual fires based on a new methodology to identify the location and timing of fire ignitions and estimate fire size, duration, daily expansion, fire line, speed, and direction of spread. The Global Fire Atlas is derived from the Moderate Resolution Imaging Spectroradiometer (MODIS) collection 6 burned area dataset (Giglio et al., 2018) and estimated day of burn information at 500 m resolution. Individual fire data were generated starting in 2003, when combined data from the Terra and Aqua satellites provide greater burn date certainty. The algorithm for the Global Fire Atlas tracks the daily progression of individual fires at 500 m resolution to produce a set

of metrics on individual fire behavior in standard raster and vector data formats. Together, these Global Fire Atlas data layers provide an unprecedented look at global fire behavior and changes in fire dynamics during 2003-2016. The data are freely available at http://www.globalfiredata.org, and new years will be added to the dataset following the availability of global burned area data.

2 Data and Methods

Here we developed a method to isolate individual fires from daily moderate resolution burned area data. The approach used two filters to account for uncertainties in the day of burn in order to map the location and timing of fire ignitions and the extent and duration of individual fires (Fig. 1). Subsequently, we tracked the growth dynamics of each individual fire to estimate the daily expansion, daily fire line, speed and direction of spread. Based on the Global Fire Atlas algorithm, burned area was broken down into seven fire characteristics in three steps (Fig. 1b). First, burned area was described as the product of ignitions and individual fire sizes. Second, fire size was further separated into fire duration and a daily expansion component. Third, the daily fire expansion was subdivided into fire speed, the length of the fire line, and the direction of spread. The Global Fire Atlas algorithm can be applied to any moderate resolution daily global burned area product, and ~~The~~ the quality of the resulting dataset depends both on the Fire Atlas algorithm as well as the underlying burned area estimates~~MCD64A1 collection 6 burned area dataset (Giglio et al., 2018);~~ . ~~for example,~~ Here we applied the algorithm to the MCD64A1 collection 6 burned area dataset (Giglio et al., 2018) and the minimum detected fire size is therefore one MODIS pixel (21 ha). Several studies have shown that the MCD64A1 col. 6 burned area product provides a considerable improvement compared to previous generation of moderate resolution global burned area products (Padilla et al., 2015; Giglio et al., 2018; Humber et al., 2018). We also present an initial effort to validate the higher order Global Fire Atlas products using independent fire perimeter data for the continental US and active fire detections to assess estimated fire duration and the temporal accuracy of individual fire dynamics.

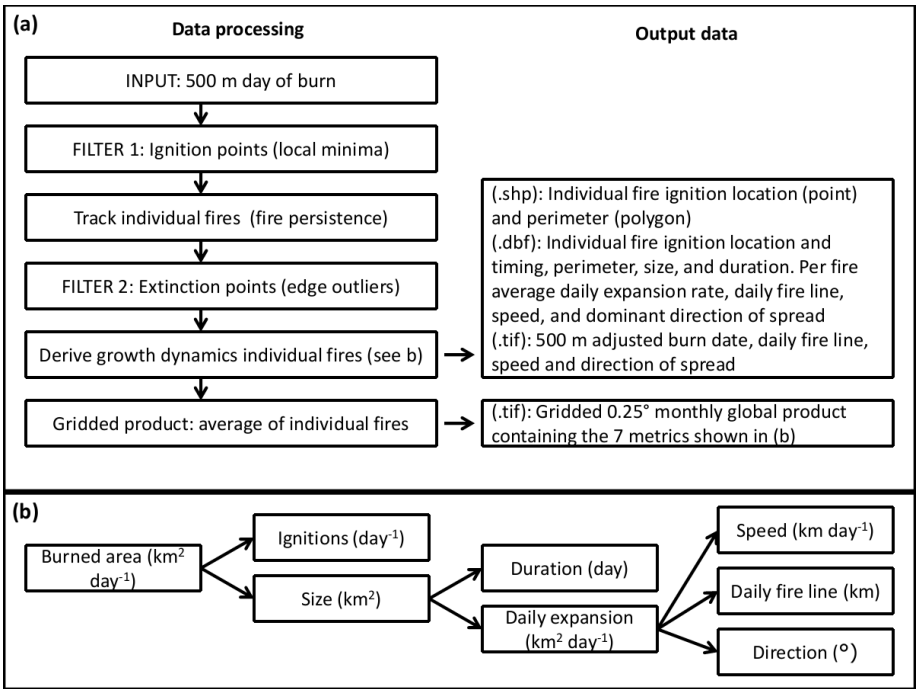

Figure 1: Flow chart showing the data-processing steps and resulting products. (a) The Global Fire Atlas algorithm tracks individual fires and their day-to-day behavior based on the MCD64A1 collection 6 500 m daily burned area product starting in 2003. (b) Decomposition of burned area into seven different

components of the fire regime in the Global Fire Atlas. The output includes two annual shape file layers (.shp) of ignition location and individual fire perimeters with corresponding database files (.dbf) providing summary information for each individual fire, including the seven key characteristics (b). In addition, four global raster maps on the 500 m sinusoidal MODIS grid (.tif) provide details on the day-to-day fire behavior. Finally, data are summarized in a monthly 0.25° gridded product based on average values of individual fires. Global Fire Atlas data-layers are described in more detail in Table A1.

2.1 Individual fires: ignitions, size, perimeter and duration

Large burn patches are often made up of multiple individual fires that may burn simultaneously or at different points in time during the burning season, particularly in frequently burning grasslands and savannas with a high density of ignitions from human activity. Separating large clusters of burned area into individual fires is therefore critical to understand the fire regime in human-dominated landscapes. To isolate individual fires, clusters of adjacent burned area for a given fire season (12 months centered on the month of maximum burned area) were subdivided into individual fires based on the spatial structure of estimated burn dates in the MCD64A1 burned area product. Although we allow individual fires to burn from one fire season into the next, we processed the data on a per-fire-season basis in each 10° x 10° MODIS tile. In the rare case a pixel burned twice during a single fire season (<1%), we retained only the earliest burn date. This approach results in a small reduction of total burned area, but allows us to produce user friendly global annual layers in both gridded and shapefile format.~~This format allowed us to create global annual 500 m data layers with minimal loss of information.~~ To locate candidate ignition points within each burned area cluster, we mapped the "local minima," defined as a single grid cell or group of adjacent grid cells with the same burn date surrounded by grid cells with later burn dates. However, because of orbital coverage and cloud cover, burn date estimates are somewhat uncertain (Giglio et al., 2013), which results in many local minima that may not correspond to actual ignition points. We applied a three-step procedure to address burn date uncertainty and distinguish individual fires. First, we developed a filter to adjust the burn date of local minima that do not correspond to ignition points. Second, we set a "fire persistence" threshold that determines how long a fire may take to spread from one 500 m grid cell into the next, to distinguish individual fires that are adjacent but occurred at different times in the burning season. Third, we developed a second filter to correct for outliers in the burn date that occurred along the edges of large fires. Each of these steps is described in detail below.

The ignition point filter is based on the assumption that the fires progress in a logical manner through space and time. First, all local minima were mapped within the original field of burn dates (Fig. 2a and b). Next, each local minimum was replaced by the nearest later burn date in time of the surrounding grid cells, and a new map of local minima was created. If the original local minimum remained as a part of a new, larger local minimum with a later burn date, the fire followed a logical progression in time and space and the original local minimum was retained. If the local minimum disappeared, the original local minimum was likely the product of an inconsistency within the field of burn dates rather than a true ignition point and the burn date was adjusted forward in time to remove the original local minimum. This step can be repeated several times, with each new iteration further reducing the number of local minima and increasing the confidence in ignition points, but, each iteration may also result in greater adjustment of the original burn date (Fig. A1). Here we implemented three iterations of the ignition point filter to remove most local minima that did not spread forward in time while limiting the scope of burn date adjustments (~~e.g.~~ Figs. 2c and d~~ and~~, A1 and A2). For short duration fires, the ignition points were retained associated with largest possible number of iterations. ~~In addition~~In all cases, if several local minima were all connected through a single cluster of grid cells with the same burn date, only the local minimum with the earliest burn date or largest number of grid cells was retained, unless the required adjustment of the burn date was larger than the specified burn date uncertainty in the MCD64A1 product. By design, the ignition point filter cannot adjust the earliest burn date of a fire, and thus has no influence on estimated fire duration.

To establish the location and date of ignition points, as well as to track the daily growth and extent of individual fires, we used a "fire persistence" threshold that determines how long a fire may take to spread from one grid cell into the next, taking both fire spread rate and satellite coverage into account (Fig. ~~A2~~A3). For example, if an ignition point was adjacent to a fire that burned earlier in the season, this threshold allowed the ignition point to be mapped as separate local minima despite the presence of adjacent burned grid cells with earlier burn dates. On the other hand, when an active fire is covered by dense clouds or smoke, multiple days can pass before a new observation can be made, resulting in a break in fire continuity and increasing the risk of artificially splitting single fires into multiple parts. Using such a threshold is particularly important to distinguish individual fires in frequently burning savannas and highly fragmented agricultural landscapes, where many individual small fires may occur within a relatively short time span. Because there are no reference datasets on global fire persistence, we used a spatially-varying fire persistence threshold that depends on fire frequency (Andela et al., 2017). We assumed that frequently-burning landscapes are generally characterized by faster fires and higher ignition densities, increasing the likelihood of having multiple ignition points within large burn patches, while infrequently burning landscapes will generally be characterized by slower fire spread rates and/or fewer ignitions. In addition, frequently burning landscapes often face a pronounced dry season characterized by low cloud cover, while infrequently burning landscapes may experience a shorter dry season with greater obscuration by clouds. Therefore, we used a 4-day fire persistence threshold for 500 m grid cells that burned more than 3 times during the study period (2003 - 2016), and a 6, 8 and 10-day fire persistence period for grid cells that burned 3 times, 2 times~~2-3, 1-2~~, or 1 time, respectively. These threshold values broadly correspond to biomes, with shorter persistence values for tropical regions and human-dominated landscapes, and longer threshold values for temperate and boreal ecosystems with high fuel loads (Fig. A2).

Based on the location and date of the established ignition points and the fire persistence thresholds, we tracked the growth of each individual fire through time to determine its size, perimeter, and duration (Fig 2f). For each day of year, we allowed individual fires to grow into the areas that burned on that specific day, as long as the difference in burn dates between two pixels was equal to or smaller than the fire persistence threshold of the pixel of origin. When two actively burning fires met each other, as on day 255 for the example fires shown in Fig. 2, grid cells that burned on the day of the merger were divided based on nearest distance to the fire perimeter on the previous day.

Burn date uncertainty may also lead to multiple "extinction points," outliers in the estimated day of burn along the edges of a fire. Environmental conditions such as cloud cover complicate the precise estimation of the date of fire extinction, as rainfall events extinguish many fires, and pixels at the edge of the fire may be partially burned and therefore harder to detect. In addition, the contextual relabeling phase of the MCD64A1 algorithm increases burn date uncertainty for extinction points based on a longer consistency threshold (Giglio et al., 2009). We used a second filtering step to adjust the burn date for extinction points, if required. Outliers were adjusted to the nearest burn date back in time, if (1) they represented a cluster no more than 1 to 4 grid cells (0.21 – 0.9 km^2) along the edge of a fire that was as least 10 times larger and (2) the difference in burn dates was larger than the fire persistence threshold of the adjacent grid cells and thus mapped as a new fire along the edge of the larger fire. If these criteria were met, the outliers were adjusted to the nearest burn date back in time, and incorporated within the larger neighboring fire. However, if these criteria were not met (e.g., for burned areas larger than 4 grid cells), the original burn dates and ignition points were left unadjusted, resulting in separate fires. For the example fires shown in Fig. 2, the adjustment of these outliers affected four grid cells (Fig. 2e) and effectively reduced the number of ignition points (and resulting individual fires) from five (Fig. 2d) to two (Fig. 2f). After adjusting these outliers (extinction points), and including them within the larger fires, we estimated the size (km^2), duration (days) and perimeter (km) of each individual fire based on the adjusted burn dates.

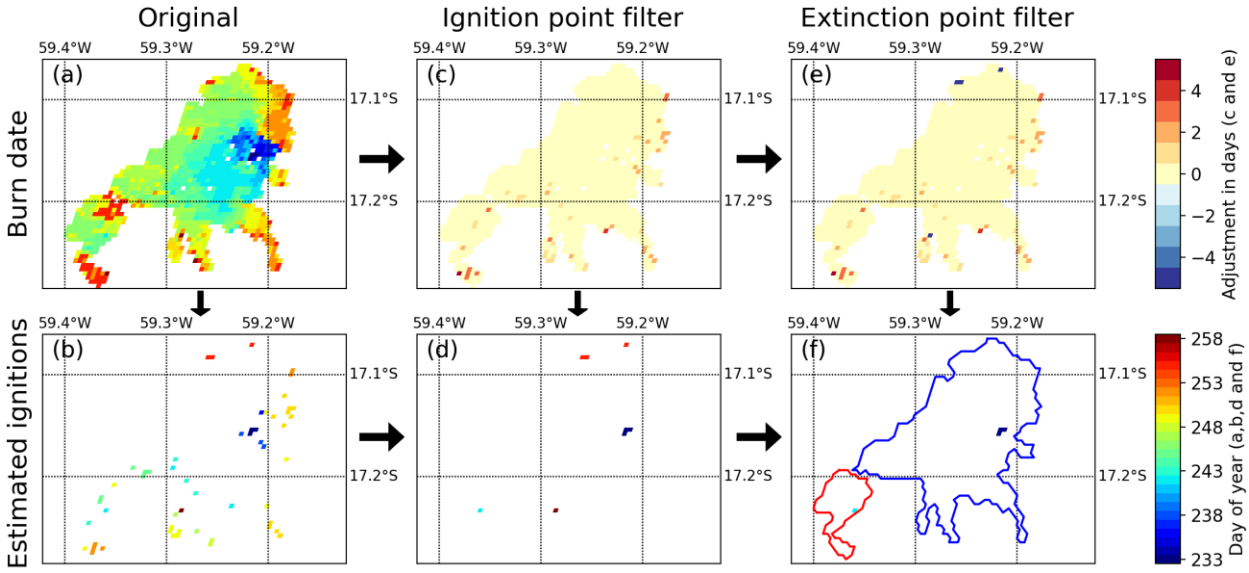

Figure 2: Example of the algorithm to account for uncertainty in the "day of burn" and identify individual fires within large clusters of adjacent burned pixels. (a) The original MCD64A1 collection 6 day of burn for one burnt patch in the Brazilian Cerrado (2015), and (b) local minima or "ignition points" identified within the original day of burn field. (c) Burn date adjustment based on the filter that removes local minima that do not progress continuously through time and space (positive adjustment), and (d) the corresponding estimate of ignition points based on the adjusted day of burn field. (e) Further burn date adjustment based on the removal of outliers along the edge of the fire (negative adjustment of extinction points), and (f) the final estimate of ignition locations and date by the Global Fire Atlas based on the combined adjustments shown in (e). In (f), the colored lines indicate the final estimates of fire perimeters.

2.2 Daily fire expansion: fire line, speed, and direction of spread

The revised day of burn estimates were used to track the daily expansion (km^2 day^{-1}) and length of the fire line (km) for each individual fire. The daily estimates of fire line length were based on the daily perimeter of the fire, where we assumed that once the fire reaches the edge of the burn scar, this part of the perimeter stops burning after one day (Fig. 3a). The expansion of the fire (km^2 day^{-1}) is the area burned by a fire each day. The average speed of the fire line (km day^{-1}) can now be calculated as the expansion (km^2 day^{-1}) divided by the length of the fire line (km) on the same day. However, this estimate of fire line includes the head, flank and backfire, while it is typically the head-fire that moves fastest and may be responsible for most of the burned area. Moreover, fire dynamics tend to be highly variable in space and time. To understand the spatial variability and distribution of fire speeds, we therefore used an alternative method to estimate the speed and direction of fire spread for each individual 500 m grid cell.

To estimate the speed and direction of spread (Fig. 3), we calculated the "most likely" path of the fire to reach each individual 500 m grid cell based on shortest distance. More specifically, for each grid cell we estimated the shortest route to connect the grid cell between two points: 1) the nearest point on the fire line with the same day of burn and 2) the nearest point on the previous day's fire line. This route was forced to follow areas burned on the specific day. For each point on this route, or "fire path," the speed of the fire (km day^{-1}) was estimated as the length of the path (km) divided by one day (day^{-1}) and the direction as the direction of the next grid cell on the fire path. Since each grid cell is surrounded by 8 other grid cells, this resulted in eight possible spread directions: north, northeast, east, southeast, south,

southwest, west, and northwest. For ignition points that represented a cluster of 500 m grid cells with the same burn date, we assumed that the fire originated in the center point of the cluster (pixel with largest distance to the final fire perimeter by the end of day 1) and spreads towards the perimeter of the fire by the end of day 1 over the course of one day. For single pixel fires, we assumed the fire burned across 463 m (1 pixel) during a single day and we did not assign a direction of spread. Similarly, fires of all sizes that burned on a single day were not assigned a direction of spread. We corrected estimates of both speed and direction for the orientation between 500 m grid cells on the MODIS sinusoidal projection that varies with location. When a particular grid cell formed part of multiple "fire paths," the earliest time of arrival or the highest fire speed and corresponding direction of spread were retained. This assures a logical progression of the fire in time and space and corresponds to fires typically moving fastest in a principal direction and then spreading more slowly along the flank.

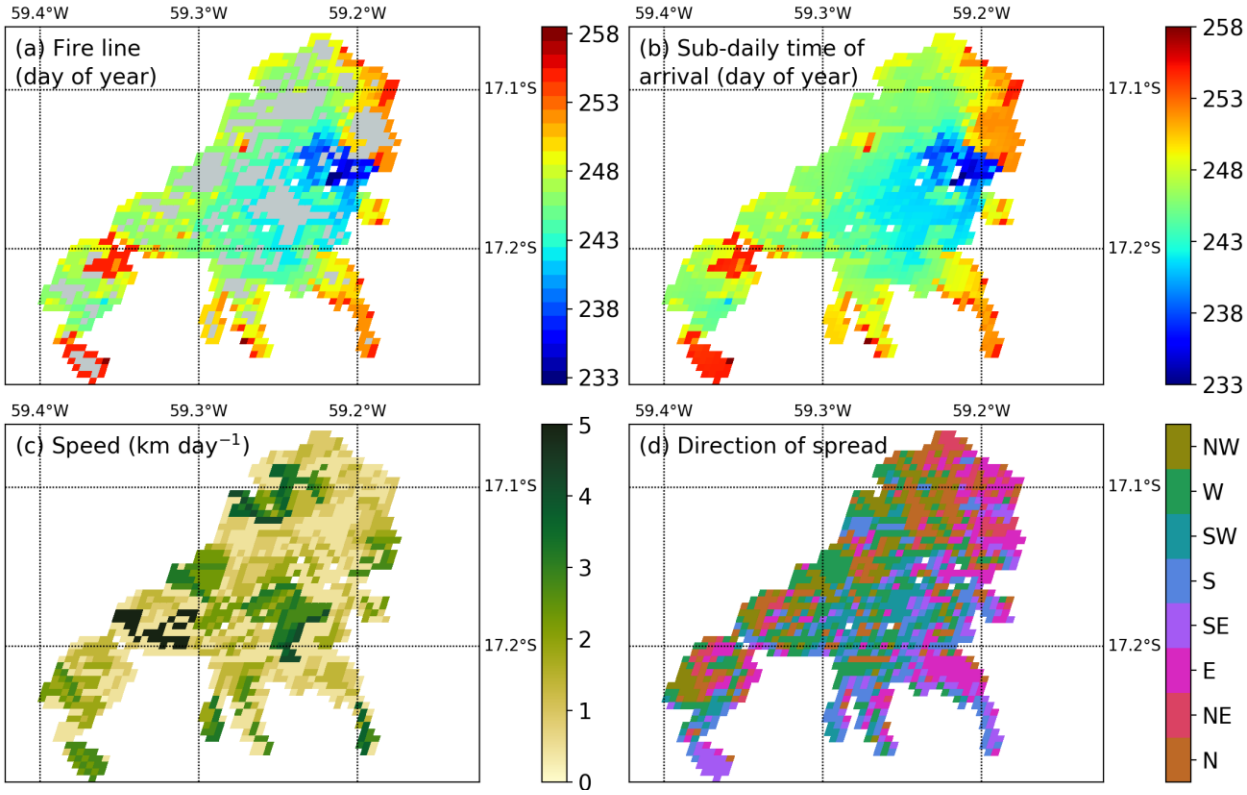

Figure 3: Sub-daily estimates of fire progression can be used to estimate spatiotemporal variation in fire speed and direction of spread. (a) daily progression of the fire line, (b) interpolated estimates of sub-daily time of arrival, (c) fire speed (km day^{-1}), and (d) direction of spread. The light gray areas in (a) are burned areas between fire lines and correspond to areas of relatively high fire speed. White areas were not burned.

2.3 Validation

Few large-scale datasets are available on daily or sub-daily fire dynamics, highlighting the novelty of the Global Fire Atlas dataset but also posing challenges for validation. Here we used two alternative datasets for this purpose. First, we used active fire detections to assess the temporal accuracy of the Global Fire Atlas burn date. Second, we compared fire perimeters to independent fire perimeter data for the continental US. ~~Finally~~ Third, we combined the independent data on fire perimeters with active fire detections to evaluate the Global Fire Atlas fire duration estimates. Finally, we compared Global Fire Atlas data to a small (manually compiled) dataset of daily fire perimeters from the US Forest Service.

We used the 375 m resolution active fire detections (VNP14IMGML C1) derived from the Visible Infrared Imaging Radiometer Suite (VIIRS) instrument aboard the Suomi National Polar-orbiting Partnership (Suomi-NPP) satellite (Schroeder et al., 2014). Active fire detections provide accurate information on the burn date, particularly in ecosystems with low fuel loads where fires will typically be active during only a single day in each particular grid cell. We compared the date of active fire detections from VIIRS within each larger 500 m MODIS grid cell (based on VIIRS center point) to the adjusted MCD64A1 day of burn to understand the temporal precision of the derived Global Fire Atlas products. If several active fire detections were available for a single 500 m MODIS grid cell we used the date closest to the mean. We compared all 500 m MODIS grid cells with corresponding active fire detection during the overlapping data period (2012 – 2016) for four different ecosystems globally: (1) forests (including all forests), (2) shrublands (including open and closed shrublands), (3) woody savannas and (4) savannas and grasslands, with land cover type derived from MODIS MCD12Q1 collection 5.1 data for 2012 using the University of Maryland (UMD) classification (Friedl et al., 2002).

We compared fire perimeters from the Global Fire Atlas to fire perimeter estimates from the Monitoring Trends in Burn Severity (MTBS) project during their overlapping period (2003 – 2015). The MTBS project provides semi-automated estimates of fire perimeters based on 30 m Landsat data for fires with a minimum size of 1000 acres (405 ha) in the western US and 500 acres (202 ha) in the eastern US (Eidenshink et al., 2007; Sparks et al., 2015). In order to determine overlap between MTBS and Fire Atlas perimeter estimates, we rasterized the MTBS perimeters onto the 500 m MODIS sinusoidal grid including all 500 m grid cells with their center point within the higher resolution (30 m) MTBS fire perimeter. For all overlapping fire perimeters, we compared the original MTBS fire perimeter information with the Fire Atlas estimates of fire perimeters. In cases with multiple overlapping perimeters, fires with the largest overlapping surface area were compared.

We also combined MTBS fire perimeters with VIIRS active fire detections to derive an alternative estimate of fire duration (2012 – 2015). In order to determine the fire duration, we first determined the median burn date of each fire according to the MCD64A1 burned area data. Subsequently, we included all VIIRS active fire detections before and after the median or 'center' burn date until a period of three fire-free days was reached. Any active fire detections that occurred outside this timeframe were excluded to avoid overestimation of the fire duration due to smoldering or possible false detections before or after the fire. Two thresholds were used to select a subset of MTBS and Fire Atlas perimeters for validation of estimated fire duration. Fires were first matched based on perimeters, with maximum of a threefold difference between perimeters. Second, we further selected MTBS perimeters with VIIRS active fire detections for at least 25% of the 500 m Fire Atlas grid cells. These thresholds excluded 51% of the overlapping fire perimeters, but reduced errors originating from cloud cover or differences in the underlying burned area estimates (e.g., resolution, methodology) to evaluate estimated fire duration. Similar to the burn date validation, comparisons of fire perimeters and fire duration with MTBS data over the continental US were grouped into four land cover types: (1) forests, (2) shrublands, (3) woody savannas and (4) savannas and grasslands.

For specific large wildfires across the western USA, the US Forest Service National Infrared Operations (NIROPS; https://fsapps.nwcg.gov/nirops/) derives estimates of daily fire perimeters for fire management purposes by collecting night-time high resolution infrared imagery. This imagery is manually analyzed by trained specialists to extract the active fire front. Although these data provide a wealth of information, only few fires were completely and precisely documented. From their database we were able to extract 15 large fires for which daily perimeter information was available. Although insufficient for full scale validation, results provide valuable insights into the strengths and shortcomings of the Global Fire Atlas estimates of individual fire size, duration and expansion rates. In addition, we compared day-to-day expansion rates (km^2 day^{-1}) of individual large fires across both datasets. If multiple Global Fire Atlas

perimeters overlapped with a single US Forest Service fire perimeter, we compared the fires with the largest overlapping surface area.

3 Results

3.1 Validation

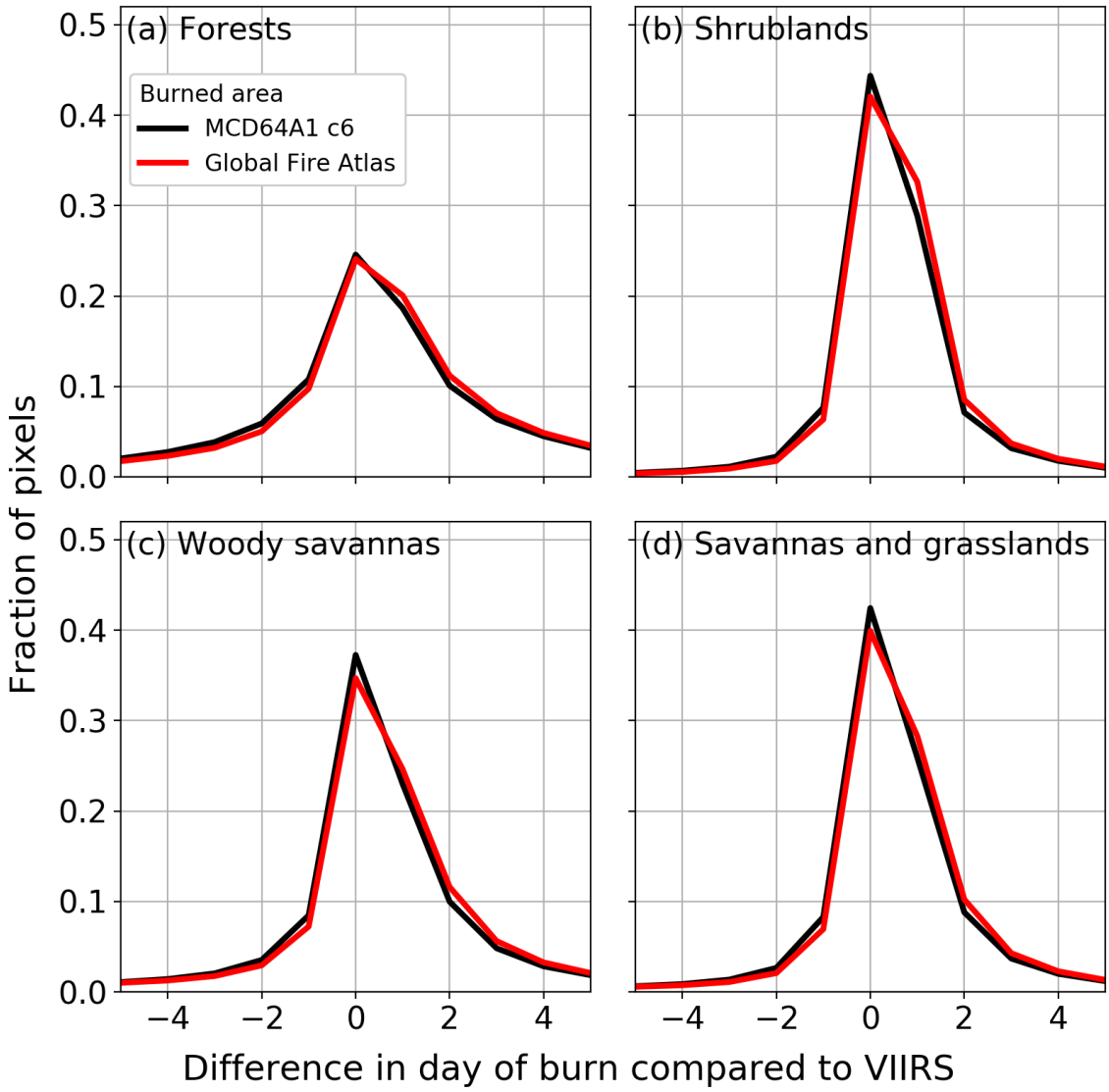

Figure 4: Per pixel global ~~Comparison~~ comparison of burn dates derived from the MCD64A1 burned area product, adjusted burn dates of the Global Fire Atlas, and VIIRS active fire detections (2012 – 2016). (a) Forests, (b) shrublands, (c) woody savannas, and (d) savannas and grasslands. Negative values indicate pixels with a burned area day of burn earlier than the first corresponding VIIRS active fire detection, zero indicates no difference in day of burn between both datasets, and positive numbers indicate a delayed detection of burned area compared to active fire detections.

At the pixel scale, estimated burn dates from burned area and active fire products were comparable (Fig. 4), with greater variability across biomes than from minor burn date adjustments in the Global Fire Atlas algorithm. Burn dates estimated from MODIS burned area and VIIRS active fire detections were least comparable in high-biomass ecosystems with lower fire spread rates. In forests and woody savannas 24% and 35% of burned pixels were detected on the same day and 54% and 67% within ± 1 day, respectively

(Fig. 4a and c). With decreasing biomass, the direct correspondence between burn dates from burned area and active fire detections increased to 41% (same day) and 80% (± 1 day) in shrublands (Fig. 4b) and 40% (same day) and 75% (± 1 day) in savannas and grasslands (Fig. 4d). These differences likely stem from the combined increase in uncertainty of burn date in higher-biomass ecosystems and influence of fire persistence (multiple active fire days in a single 500 m grid cell) on the ability to reconcile the timing of burned area and active fire detections in these ecosystems. Several factors may account for the positive bias in the 500 m day of burn from burned area compared to active fire detections, including orbital coverage, cloud and smoke obscuration, and different thresholds between burned area and active fire algorithms regarding the burnt fraction of a 500 m grid cell. The adjustments made to the burn date here, required to effectively determine the extent and duration of individual fires, had a relatively small effect on the overall accuracy but tended to reduce the negative bias in burn dates and increase the positive bias (i.e. delayed burn date compared to active fire detection, see red and black lines in Fig 4). In line with these findings, we found good agreement between a 3-day running average of Global Fire Atlas and US Forest service estimates of daily fire expansion, but reduced correspondence for daily estimates of fire growth rates due to uncertainty in the day-of-burn of the burned area product (Fig. B1).

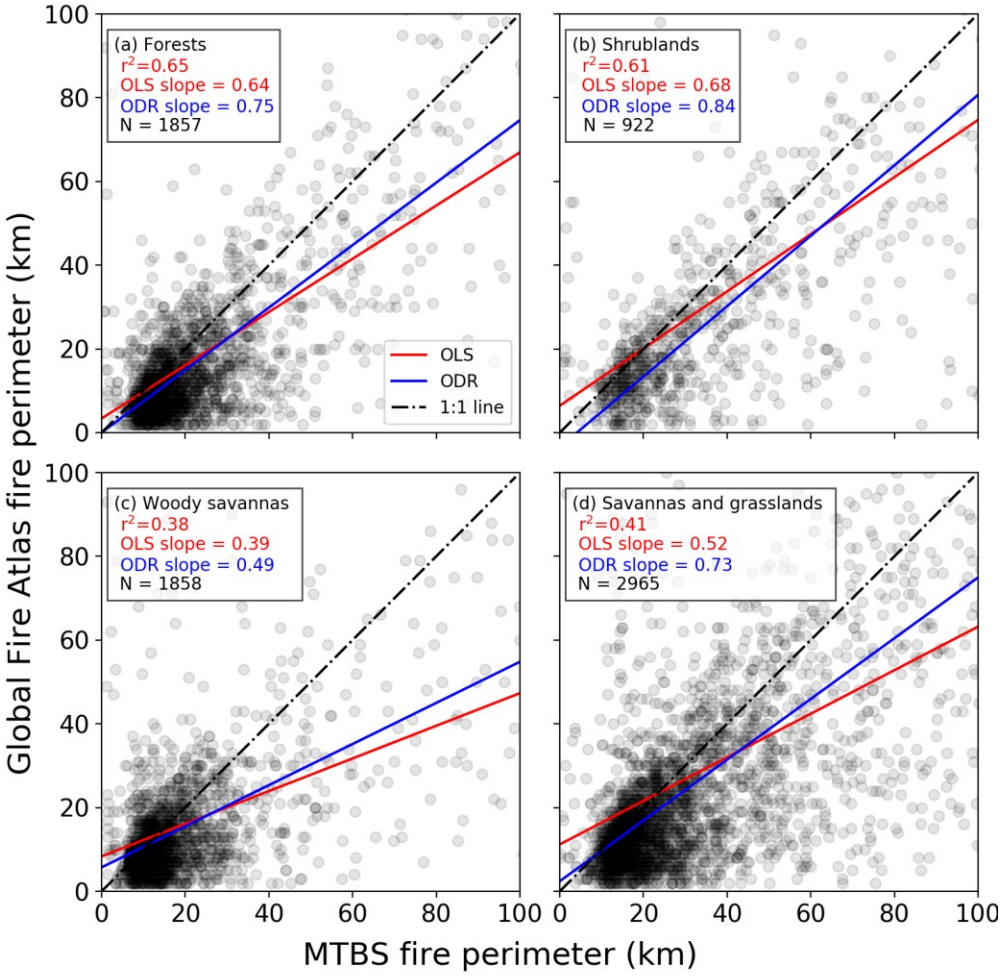

Figure 5: Comparison of fire perimeter estimates based on the Global Fire Atlas and MTBS for the continental US (2003 – 2015). (a) Forests, (b) shrublands, (c) woody savannas, and (d) savannas and grasslands. Red lines indicate the slope between both datasets based on ordinary least squares (OLS) with corresponding r^2 values, while blue lines are based on orthogonal distance regression (ODR). For the scatter plots, darker gray or black indicates a greater density of points.

For fire perimeters, the best agreement between the Global Fire Atlas and MTBS was found in forests and shrublands, where the Global Fire Atlas reproduced 65% and 61% of the observed variance in MTBS fire perimeters, respectively (Fig. 5). Less agreement was found for woody savannas (38%) and savannas and grasslands (41%). However, uncertainty exists in both datasets. Orthogonal distance regression (ODR) accommodates uncertainties in both datasets and generally resulted in slopes closer to the 1:1 line, indicating closer correspondence, on average, in absolute perimeter estimates for the two datasets. An in-depth comparison of the performance of the Global Fire Atlas and the MTBS datasets for several grassland fires in Kansas (USA) suggested that differences originated both from the underlying burned area datasets and the methodologies (Fig. ~~B1~~B2). For this particular grassland in Kansas, the MCD64A1 product estimated less burned area compared to the Landsat-based MTBS dataset, resulting in fragmentation of larger burn scars into disconnected patches. However, the daily temporal resolution of the MCD64A1 burned area product allowed for recognition of individual ignition points within larger burn patches of fast moving grassland fires that cannot be separated using infrequent Landsat imagery (Fig. B2). In addition, the 30 m spatial resolution of the MTBS perimeters may result in more irregularity and therefore in longer fire perimeter estimates compared to the 500 m Fire Atlas perimeters ~~(Fig. B1)~~. Combined, these tradeoffs in spatial and temporal resolution resulted in less agreement between fire perimeters in woody savannas (Fig. 5c) and savannas and grasslands (Fig. 5d).

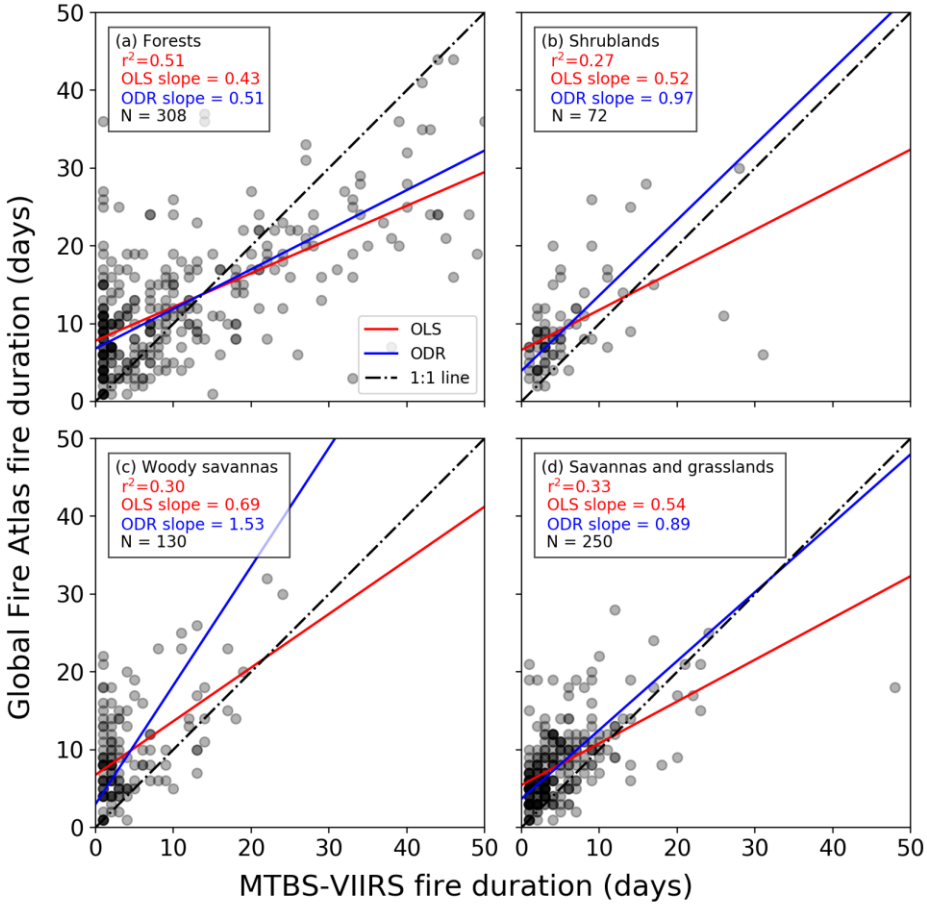

Figure 6: Comparison of fire duration estimates from the Global Fire Atlas and the combination of VIIRS active fire detections within MTBS fire perimeters for the continental US (2012 – 2015). (a) Forests, (b) shrublands, (c) woody savannas, and (d) savannas and grasslands. Red lines indicate the slope between both datasets based on ordinary least squares (OLS) with corresponding r^2 values, while blue

lines are based on orthogonal distance regression (ODR). For the scatter plots, darker gray or black indicates a greater density of points. This comparison used a subset of MTBS and Fire Atlas perimeters based on selection criteria for perimeter overlap and VIIRS active fire detections (see Section 2.3).

Initial validation of fire duration estimates from the Global Fire Atlas highlighted the differences in the sensitivity of satellite-based burned area and active fire products to fire lifetime (Fig. 6). Similar to fire perimeters, the best agreement in fire duration estimates was found for forests, where the Global Fire Atlas reproduced 51% of the observed variance of the fire duration estimates based on combining MTBS fire perimeters with active fire detections. Shrublands, woody savannas, and savannas and grasslands had lower correlations, with 27%, 30% and 33% of the variance explained, respectively. The orthogonal distance regression resulted in slopes close to the one-to-one line for shrublands and savannas and grasslands, indicating reasonable agreement. Fire duration was clearly underestimated for forested ecosystems with high fuel loads, as fires may continue to smolder for days (resulting in active fire detections) after the fire has stopped expanding.

The comparison of Global Fire Atlas data to a small dataset (n = 15) of daily perimeters of large wildfires in primarily forested cover types mapped by the US Forest Service yielded good correspondence between estimates of fire size, duration, and expansion rates (Fig. 7). The improved comparison of fire size (cf. Fig. 5a and 7a) could be related to the US Forest Service data being more accurate than MTBS, but likely also represents the good performance of the Global Fire Atlas (e.g. compare Figs. 7a, b and c to Figs. 7d, e and f) and underlying burned area products (Fusco et al., 2019) for relatively large fires. In contrast to the suggested underestimate of fire duration shown in Fig. 6a, these data suggest the Global Fire Atlas may slightly overestimate fire duration. This difference may reflect the fact that active fire detections may be triggered by smoldering while the burned area product will only register the initial changes in surface reflectance from fire. Based on a small underestimate of overall burned area and overestimate of fire duration by the Global Fire Atlas, the average daily fire expansion rates based on US Forest Service data were higher than estimates based on Global Fire Atlas data (Fig. 7c and f).

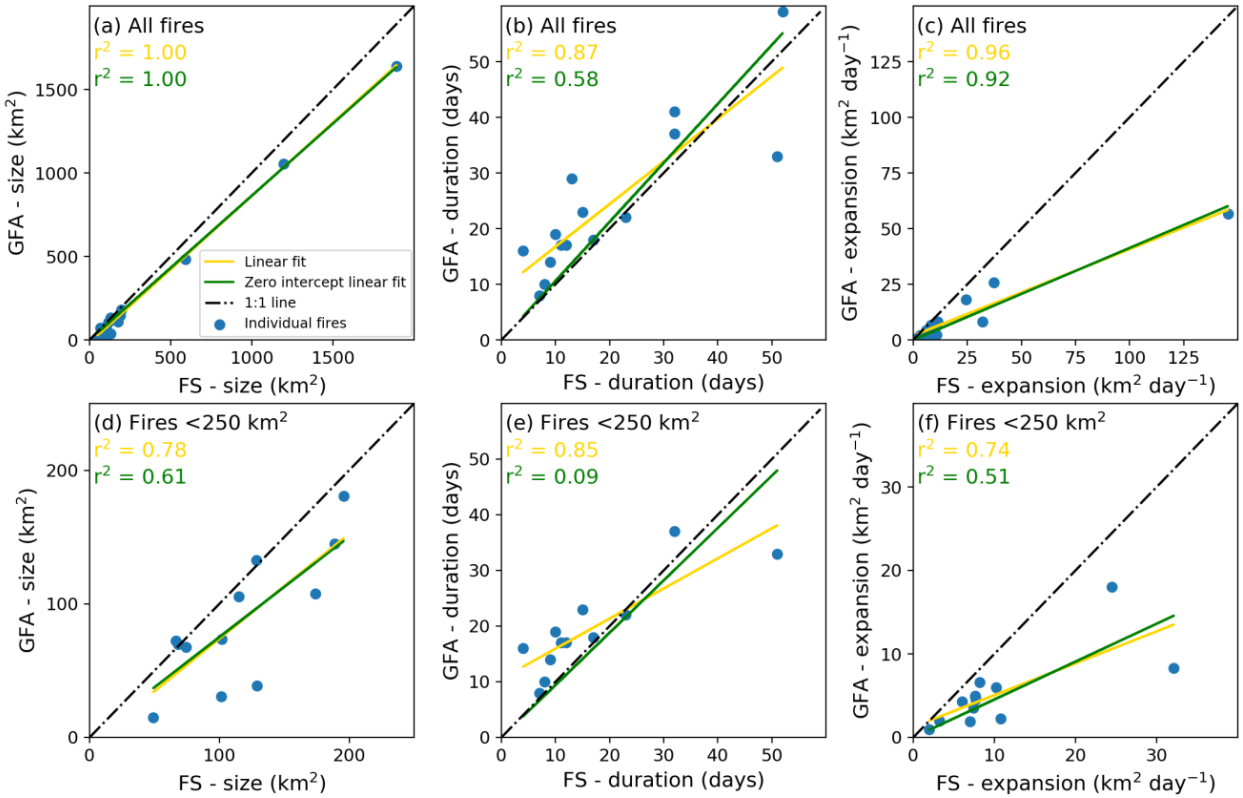

Figure 7: Comparison of Global Fire Atlas (GFA) and US Forest Service (FS) data for a selected number of large wildfires in the US. Comparison of (a) fire size, (b) duration, and (c) average daily expansion rate for all fires (N=15), (d, e and f) are like (a, b and c) but for fires smaller than 250 km^2 (N=12). Correlation coefficients are provided based on linear regression with (yellow) and without (green) intercept, assuming a non-zero intercept could indicate a structural offset between both datasets.

3.2 Characterizing global fire regimes

Over the 14-year study period we identified 13,250,145 individual fires with an average size of 4.4 km^2 (Table 1) and minimum size of one MODIS pixel (21 ha or 0.21 km^2). On average, largest fires were found in Australia (17.9 km^2), boreal North America (6.0 km^2), and northern hemisphere Africa (5.1 km^2), while central America (1.7 km^2), equatorial Asia (1.8 km^2), and Europe (2.0 km^2) had the smallest average fire sizes (Table 1). Spatial patterns of number of ignitions and fire sizes were markedly different and often inversely related (Fig. ~~7~~8). Burned area in agricultural regions and parts of the humid tropics, particularly in Africa, resulted from high densities of fire ignitions and relatively small fires, consistent with widespread use of fire for land management. Large fires accounted for most of the burned area in arid regions, high latitudes, and other natural areas with low population densities and a sufficiently long season of favorable fire weather (Fig. ~~7~~8).

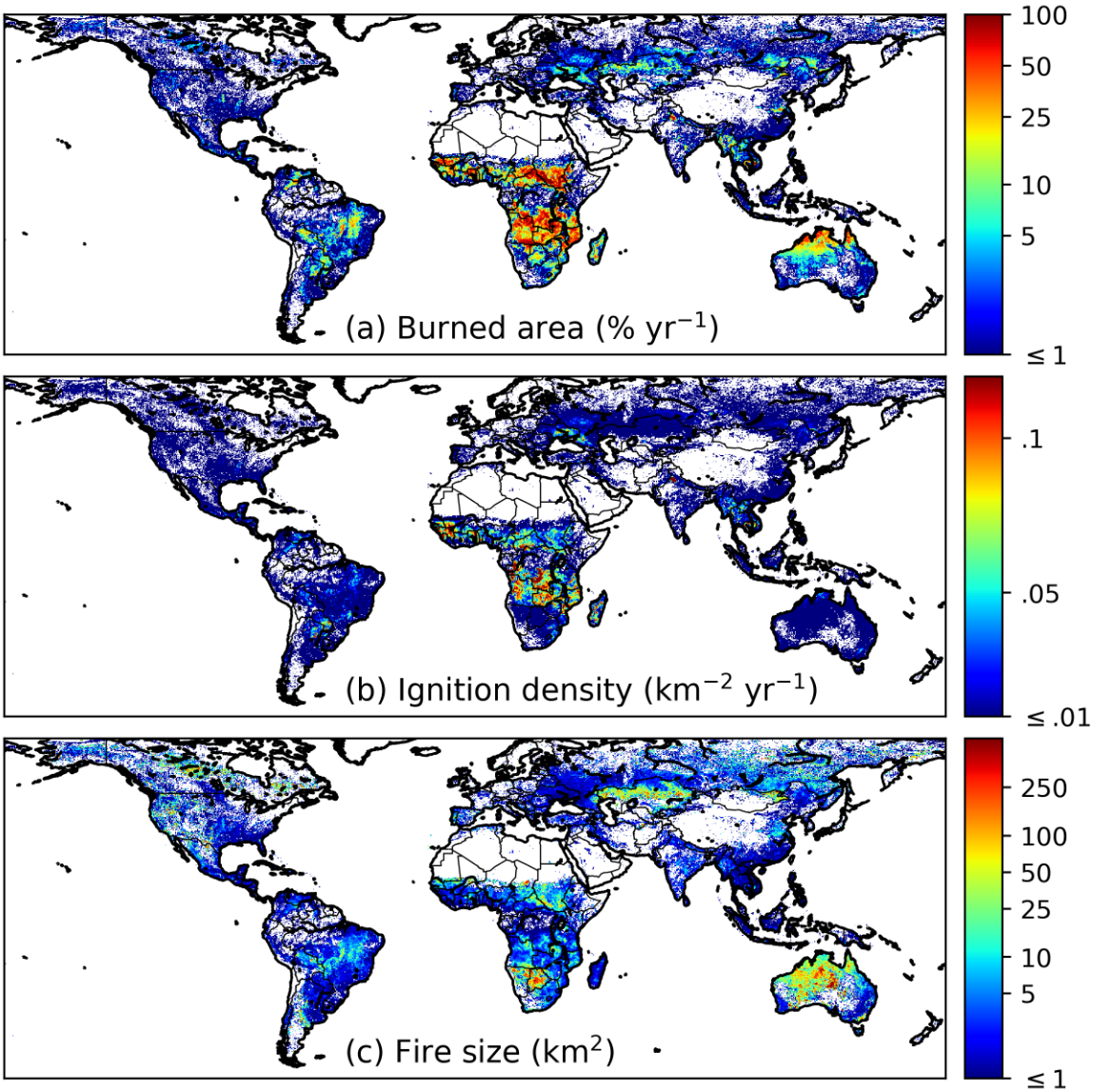

Figure ~~7~~8: Average global burned area (MCD64A1), ignition density, and fire size over the study period 2003 – 2016. For any given area (a) ~~Burned~~ burned area in km^2 per year ~~is~~ would be the product of (b) ignitions per year and (c) fire size in km^2. However, because the size of a 0.25° grid cell varies with latitude we have converted the units of burned area to fraction (%) per year and of ignitions to number per km^2 per year for spatial consistency.

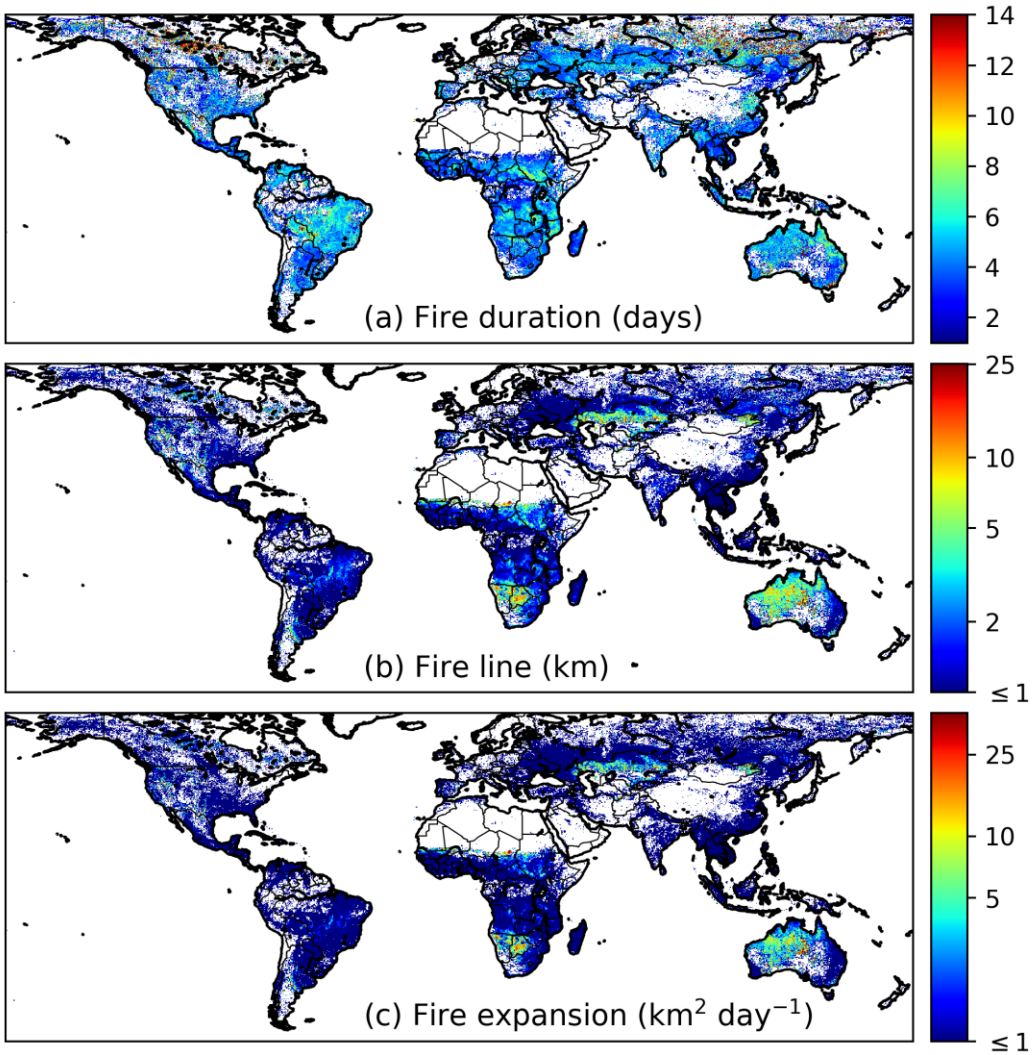

Figure ~~8~~9: Average fire duration (a), fire line length (b), and daily expansion (c) over the study period 2003 – 2016. Fire size (see Fig. 7c) is the product of fire duration (a) and daily fire expansion (c).

Global patterns of fire duration and expansion rates provide new insights in the occurrence of large fires, as the size of each fire (km^2) is the product of fire duration (days) and daily fire expansion rate (km^2 day^{-1}). Individual fires that burned for a week or more occurred frequently across the productive tropical grasslands and in boreal regions (Fig. ~~8a~~9a, Table 2). In these regions, fire duration exerted a strong control on fire size and total burned area. On average, human-dominated landscapes such as deforestation frontiers or agricultural regions experienced smaller and shorter fires compared to natural landscapes (Table 2). Fire duration was also relatively short in semiarid grasslands and shrublands characterized by high daily fire expansion rates, based on the development of long fire lines (Fig. ~~8b~~ 9b and c) and high velocity. In these regions, fire duration and size were likely limited by fuel connectivity. In line with these findings, largest average daily expansion rates were found in Australia (1.7 km^2 day^{-1}), northern hemisphere Africa (0.9 km^2 day^{-1}) and southern hemisphere Africa (0.9 km^2 day^{-1}), and smallest expansion rates in central America (0.3 km^2 day^{-1}), equatorial Asia (0.3 km^2 day^{-1}), and southeast Asia (0.4 km^2 day^{-1}; Table 1).

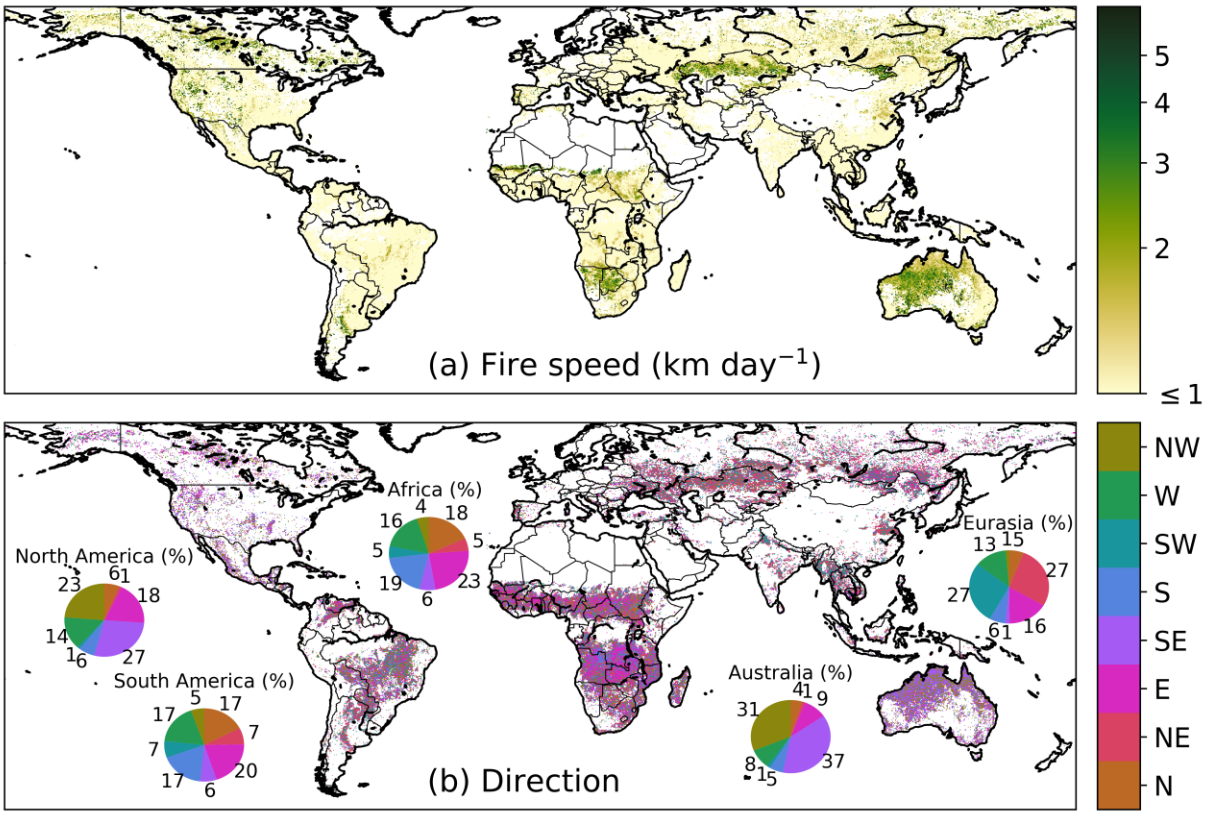

Figure ~~9~~10: Average speed of the fire (a) and the dominant direction of fire spread (b) over the study period 2003 – 2016. For each 0.25° grid cell the direction was estimated as the dominant fire spread direction of fires larger than 10 km^2 within the grid cell. We focused on larger fires (≥ 10 km^2) to determine the dominant spread direction, because large fires will generally express a clearer spatiotemporal structure of fire spread at 500 m daily resolution. Pie charts show the fraction of individual larger fires (≥ 10 km^2) by dominant spread direction for each continent.

The fastest fires occurred in arid grasslands and shrublands (Fig. ~~9~~10a), where fuel structure, climate conditions, and emergent properties of large wildfires contribute to high fire spread rates. Relatively high fire speeds were also observed in some parts of the boreal zone, particularly in central and western Canada. Lowest fire velocities were observed in infrequently burning humid tropical regions where fire spread was influenced by higher fuel loads and humidity (Table 1). At all scales, estimated fire direction exhibited considerable complexity (Fig. ~~9b~~10b). With some regional exceptions, no clear dominant spread direction was found in South America or Africa. Based on the underlying 500 m data layers, landscape structure and drainage patterns played an important role in controlling individual fire spread direction in the humid tropics. Fire spread direction also varied considerably within individual fires, and the dominant direction typically represented less than half of the pixels. Fire spread direction was more consistent in the arid tropics, as demonstrated by the northwest and southeast orientation of fire spread in Australia, consistent with the dominant wind directions. At mid-latitudes, we found evidence for more east and westward fire progression in Europe and Asia and northwest and southeast spread direction in North America, broadly consistent with the orientation of mountain ranges and other topographic features within the key biomass burning regions.

Table 1: Fire attributes for each Global Fire Emissions Database (GFED) region during 2003 – 2016. Ignitions are the summed ignitions over the study period (2003 – 2016). For size, duration, expansion, and speed the mean values are shown for individual fires and weighted by fire size (between parenthesis). For ignitions, regions with over one million ignitions are shown in red and lower values in blue, for other fire aspects values equal to or above the global average are shown in red and below the global average in blue. A map of the GFED regions is shown in the annex material (Fig. ~~B2a~~B3a).

GFED Region	Ignitions (2003-2016)	Size (km^2)	Duration (days)	Expansion (km^2 day^{-1})	Speed (km day^{-1})
World	13250145	4.4 (395.9)	4.5 (14.7)	0.6 (14.5)	0.9 (3.2)
BONA	57613	6.0 (202.8)	5.4 (23.3)	0.5 (6.8)	1.0 (4.3)
TENA	137900	2.9 (136.7)	4.7 (13.4)	0.5 (8.8)	0.8 (3.7)
CEAM	229245	1.7 (28.3)	4.3 (12.2)	0.3 (1.5)	0.7 (1.4)
NHSA	242359	3.1 (50.1)	5.1 (12.4)	0.5 (3.3)	0.8 (2.1)
SHSA	1320177	3.0 (90.6)	4.7 (13.8)	0.5 (4.8)	0.7 (2.3)
EURO	71233	2.0 (30.7)	4.6 (10.3)	0.4 (2.7)	0.7 (2.0)
MIDE	86783	2.3 (22.0)	4.0 (9.8)	0.5 (2.1)	0.8 (1.9)
NHAF	3517808	5.1 (186.2)	4.4 (14.7)	0.7 (8.6)	0.9 (3.0)
SHAF	5000436	4.3 (232.5)	4.5 (13.5)	0.7 (9.6)	0.9 (2.6)
BOAS	363279	3.7 (116.8)	4.5 (15.6)	0.5 (6.8)	1.0 (4.1)
CEAS	807739	3.2 (339.7)	4.2 (11.5)	0.5 (22.7)	0.8 (5.6)
SEAS	937810	2.2 (27.8)	4.1 (13.2)	0.4 (1.8)	0.7 (1.8)
EQAS	117870	1.8 (13.5)	5.5 (16.4)	0.3 (0.8)	0.7 (1.3)
AUST	358807	17.9 (2030.6)	5.0 (20.5)	1.7 (59.5)	1.2 (6.1)

Table 2: Fire attributes by GFED fire type during 2003 – 2016. Ignitions are the summed ignitions over the study period (2003 – 2016). For size, duration, expansion, and speed, the mean values are shown for individual fires and weighted by fire size (between parenthesis). For agriculture, we only included fires with >90% of burned area classified as cropland. For ignitions, fire types with over one million ignitions are shown in red and lower values in blue, for other fire aspects values equal to or above the global average are shown in red and below the global average in blue. A map of the GFED fire types is shown in the annex material (Fig. ~~B2b~~B3b).

GFED fire type	Ignitions (2003-2016)	Size (km^2)	Duration (days)	Expansion (km^2 day^{-1})	Speed (km day^{-1})
All	13250145	4.4 (395.9)	4.5 (14.7)	0.6 (14.5)	0.9 (3.2)
Boreal forest	197124	5.2 (149.2)	5.4 (20.1)	0.6 (6.5)	1.0 (4.2)
Temporal forest	178909	2.5 (84.1)	4.1 (14.0)	0.4 (4.2)	0.8 (2.8)
Deforestation	909826	1.4 (28.7)	3.8 (13.7)	0.3 (1.4)	0.6 (1.4)
Savanna	9809719	5.1 (447.5)	4.6 (14.9)	0.7 (16.2)	0.9 (3.4)
Agriculture	1631918	1.4 (26.4)	3.4 (10.3)	0.3 (2.0)	0.7 (1.9)

3.3 Fire extremes

The world's largest individual fires were mostly found in sparsely populated arid and semiarid grasslands and shrublands of interior Australia, Africa, and central Asia (Fig. ~~10a~~11a). Strikingly, fires of these proportions were nearly absent in North and South America, possibly due to higher landscape fragmentation and different management practices, including active fire suppression. In arid regions of

Southern Africa and Australia, large fires typically followed La Niña periods (e.g., 2011 and 2012), when increased rainfall and productivity increase fuel connectivity (Chen et al., 2017). The largest fire in the Global Fire Atlas occurred in northern Australia, burning across 40,026 km^2 (about the size of Switzerland or the Netherlands) over a period of 72 days with an average speed of 19 km day^{-1}, following the 2007 La Niña. The longest fires burned for over 2 months in seasonal regions of the humid tropics and high-latitude forests (Fig. ~~10b~~11b). Drought conditions in 2007 and 2010 caused multiple fires to burn synchronously for over two months across tropical forests and savannas in South America. Highest fire velocities typically occurred in areas of low fuel loads. While fires larger than 2500 km^2 were nearly absent from arid grass and shrublands in the North and South America, patterns of extremely fast-moving fires in arid grass and shrublands were similar to other continents. Fast-moving fires also show evidence of synchronization, for example with several extremely fast fires burning across the steppe of eastern Kazakhstan during 2003 (Fig. ~~10c~~11c).

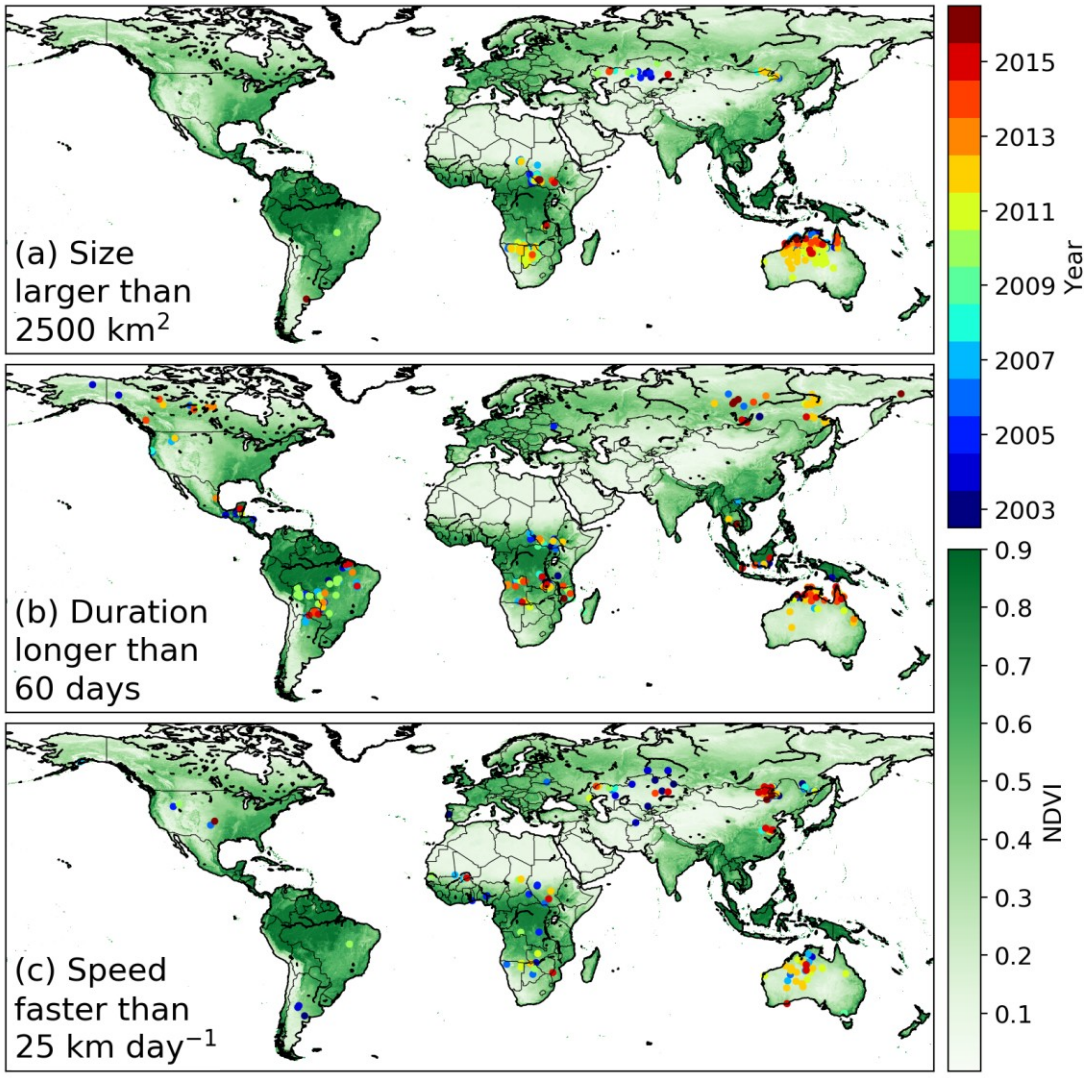

Figure ~~10~~11: Location and year of the largest, longest, and fastest fires over the study period 2003 – 2016. (a) fires larger than 2500 km^2, (b) fires longer than 60 days, and (c) fires with an average velocity larger than 25 km day^{-1}. The background image depicts mean MODIS normalized difference vegetation index (NDVI, 2003 – 2016), an indicator for large scale vegetation patterns and available fuels.

4 Discussion

The Global Fire Atlas is the first freely available global dataset to provide daily information on seven key fire characteristics: ignition timing and location, fire size, duration, daily expansion, daily fire line, speed and direction of spread based on moderate resolution burned area data. Over the 2003 – 2016 study period, we identified nearly one million individual fires (≥ 21 ha) each year (Table 1). Characteristics of these fires varied widely across ecosystems and land use types. In arid regions and other fire-prone natural landscapes, most of the burned area resulted from a small number of large fires (Fig. ~~7~~8). Fire sizes declined along gradients of increasing rainfall and human activity, with larger numbers of small fires in the humid tropics or other human-dominated landscapes. Multiday fires were the norm across nearly all landscapes, with some large fires in productive tropical grasslands and boreal regions burning for over two months during drought periods (Fig. ~~10~~11). The dominant control on fire sizes also varied across ecosystems; fire duration was the principal control on fire sizes in boreal forests, whereas fuels limited the size of fast-moving fires in arid grasslands and shrublands (Figs. ~~8~~ 9 and 10~~9~~). Characterizing fire behavior across large scales is key for understanding fire-vegetation feedbacks, emissions estimates, fire prediction, effective fire management, and modeling of fires within ecosystem models. Satellite remote sensing has been widely used to characterize global pyrogeography (Archibald et al., 2013) and fire-climate interactions (Westerling et al., 2006; Alencar et al., 2011; Morton et al., 2013a; Field et al., 2016; Young et al., 2017). Nonetheless, large-scale understanding of individual fire behavior has remained elusive without consistent global data products such as the Global Fire Atlas.

Both climate and human activity exert a strong control on global burned area (Bowman et al., 2009) and contribute to rapidly changing fire regimes worldwide (Jolly et al., 2015; Andela et al., 2017; Earl and Simmonds, 2018). Moreover, increasing human presence in fire prone ecosystems requires increased efforts to actively manage fires for ecosystem conservation and human wellbeing (Moritz et al., 2014; Knorr et al., 2016). The ignition location, spread, and duration of individual fires can be used to address new questions of fire-climate interactions and changing influence of human activity on fire behavior, as each of these aspects may respond differently to variability or change. For example, recent studies have suggested that climate warming and drying may increase fire size and burned area in the tropics (Hantson et al., 2017) and at higher latitudes (Yang et al., 2015). Our findings suggest that an increase in the length of the fire season may be the dominant driver for increases in fire activity in these ecosystems, as fire duration was a strong control on eventual fire sizes and burned area (Figs. 8~~7~~, 9~~8~~ and 1 1~~0~~). Investigating fire-climate interactions and human controls on burned area using the Fire Atlas data layers will benefit management efforts and science investigations, as fires alter vegetation structure (Bond et al., 2005; Staver et al., 2011), biogeochemical cycles (Bauters et al., 2018; Pellegrini et al., 2018) and climate (Randerson et al., 2006; Ward et al., 2012).

The Global Fire Atlas provides several new constraints that could improve the representation of fires in ecosystem and Earth system models. Fire models embedded in dynamic vegetation models are important tools for understanding the changing role of fires in the Earth system and the ecosystem impacts of fires (Hantson et al., 2016; Rabin et al., 2017). Most global models of fire activity are calibrated using satellite-derived estimates of total burned area or active fires (Hantson et al., 2016), rather than individual fire characteristics. As a result, these fire models capture the spatial distribution of global fire activity but not burned area trends (Andela et al., 2017) or interannual variability that may increase fire spread rates or duration. Models range from simple empirical schemes to complex, process-based representations of individual fires (Hantson et al., 2016; Rabin et al., 2017). Process-based models estimate burned area as the product of fire ignitions and size, while many models include a dynamic rate of spread to determine eventual fire sizes (e.g. SPITFIRE; Thonicke et al., 2010) but use arbitrary threshold values for key parameters such as fire duration (Hantson et al., 2016). We found that global patterns of fire duration, ignitions, size, and rate of spread (i.e. speed) varied widely across ecosystems and human land

management types, and thus these Global Fire Atlas data products provide additional pathways to benchmark models of various levels of complexity. While only a few models include multiday fires (e.g., Pfeiffer et al., 2013; Le Page et al., 2015; Ward et al., 2018), we found that multiday fires were the norm across most biomes, and fire duration forms an important control on eventual fire sizes and burned area in many natural ecosystems with abundant fuels. In a similar fashion, many models assume relatively homogeneous fuel beds, while our results suggest that landscape features and vegetation patterns result in highly heterogeneous fuel beds that form a strong control on fire spread (speed and direction). Large differences in fire behavior across ecosystems and management strategies may improve fire emissions estimates and emissions forecasting, particularly when combined with active fire detections to better characterize different fire stages including the smoldering phase (Kaiser et al., 2012). Recent studies have shown that fire emissions factors may vary widely depending on fire-behavior (Van Leeuwen and Van Der Werf, 2011; Parker et al., 2016; Reisen et al., 2018), while improved knowledge of fire-climate interactions are crucial for emissions forecasting (Di Giuseppe et al., 2018).

The Global Fire Atlas methodology builds on a range of previous studies that have used ~~remote sensing~~daily moderate resolution satellite imagery to estimate individual fire sizes (Archibald and Roy, 2009; Hantson et al., 2015; Frantz et al., 2016; Andela et al., 2017), shape (Nogueira et al., 2017; Laurent et al., 2018), duration (Frantz et al., 2016) and spread dynamics (Loboda and Csiszar, 2007; Coen and Schroeder, 2013; Sá et al., 2017). We provide the first fire progression-based algorithm to map individual fires across all biomes, including the first global estimates of ignition locations and timing, duration, daily expansion, fire line, speed and direction of spread. Several previous studies have estimated fire size distributions based on a flood-fill algorithm, where all neighboring pixels within a certain time threshold are classified as the same fire (Archibald and Roy, 2009; Hantson et al., 2015). Interestingly, we found similar spatial patterns of fire size (cf. Fig. 8 and Archibald et al., 2013; Hantson et al., 2015), although absolute estimates may show large differences based on the "cut off" value used within the flood-fill approach (Oom et al., 2016), and to a lesser extent by the fire persistence threshold used here. Spatial patterns of fire size and duration also compared favorably with estimates of Frantz et al. (2016) for southern Africa (Fig. ~~8a~~9a) and estimates of fire speed by Loboda et al. (2007) for central Asia (Fig. ~~9a~~10a). Here we compared our results to fire perimeter estimates from the MTBS (Eidenshink et al., 2007; Sparks et al., 2015) for validation purposes. Good agreement was found for forested ecosystems and shrublands, but results differed more in grassland biomes (Fig. 5). Interestingly, we found that the poor agreement in grasslands stemmed from differences in the spatial and temporal resolution of the burned area estimates (Fig. B2). In line with previous studies, we found that ~~While~~ the coarser resolution (500 m) of the MODIS burned area data used to develop the Global Fire Atlas sometimes underestimated overall burned area (e.g. Randerson et al., 2012; Roteta et al., 2019), ~~fragmented~~ fragmenting individual large fires~~,~~. However, the Landsat-based MTBS data at 30 m resolution were unable to distinguish individual fires within large burn patches of fast-moving grassland fires based on infrequent Landsat satellite overpasses (Fig. ~~B1~~B2).

Validation of Global Fire Atlas fire perimeter estimates for the continental US revealed several important limitations and opportunities for further development of individual fire characterization using satellite burned area data. In addition to the validation of fire perimeters, we also investigated the temporal accuracy of the Global Fire Atlas (Fig. 4) as well as the fire duration estimates (Fig. 6) based on active fire detections. Reasonable correlations (r^2 ranging from 0.3 to 0.5) were found between Global Fire Atlas and fire duration estimates based on a combination of MTBS fire perimeters and VIIRS active fire detections. Disagreement partly originated from differences in fire perimeter estimates as well as differences between the day-of-burn estimates derived from the MCD64A1 burned area data and VIIRS active fire detections. Moreover, the uncertainty in the burn date of the underlying burned area product is typically at least one day, resulting in a large uncertainty in the fire duration estimates of shorter fires. Global Fire Atlas data therefore performed best for large fires (Figs. 6 and 7). Particular care should be taken when using the Global Fire Atlas for cropland regions for two main reasons. First, mapping burned

area in croplands is notoriously difficult using moderate resolution satellite data, as typical crop residue burning is often too small to detect (Randerson et al., 2012; Giglio et al., 2013). Second, we allow a fire 4 – 10 days to spread from one grid cell into the next (fire persistence threshold), which may be more representative for natural landscapes than croplands with synchronized small fire activity at specific points in the crop cycle. The temporal accuracy of the Global Fire Atlas adjusted burned area compared to VIIRS active fire detections ranged from 41% on the same day and 80% within ± 1 day in shrublands to and 24% (same day) and 54% (± 1 day) in forests. However, in forested ecosystems the use of active fire detections for validation purposes is not ideal, as fires may smolder for days resulting in active fire detections a long time after the fire front has passed. Understanding the temporal accuracy of the Global Fire Atlas products is important for linking individual fire dynamics to fire weather, and we found good agreement between Global Fire Atlas and US Forest Service fire expansion using a 3-day running average, but less good agreement for individual days based on burn date uncertainty (Fig. B1). Other parameters, including fire speed and direction of spread, were not validated during this stage. However, our comparison to daily fire perimeter estimates from the US Forest Service show good agreement in terms of average expansion rates, suggesting reasonable overall estimates of speed (Fig. 7). Overall, there is a need to develop additional validation methodologies and data products to advance our understanding of satellite-derived estimates of individual fire behavior, building on the long-standing efforts for burned area (Boschetti et al., 2009) and active fires (Schroeder et al., 2008).

The Global Fire Atlas provides the first consistent, global assessment of individual fire behavior. Further development of the Fire Atlas product suite is possible based on improvements in the underlying burned area data, including new products at higher spatial resolution (e.g., VIIRS), and additional constraints from active fire detections. The Global Fire Atlas algorithm provides a flexible framework that can be easily adjusted to work at different spatial and/or temporal resolutions. In particular, daily burned area products do not resolve the diurnal cycle of fire activity, that may vary widely across fire regimes (Freeborn et al., 2011; Andela et al., 2015). A better understanding of the drivers of fire persistence and fuel loads across biomes and ecosystem gradients is also important.

5 Data availability

The data are freely available at http://www.globalfiredata.org in standard data product formats and updates for subsequent years will be distributed pending availability of MCD64A1 burned area data and associated research funding. Global per-fire-year shapefiles of the ignition locations (point) and individual fire perimeters (polygon) contain attribute tables with a unique fire ID, ignition location, start and end dates, size, duration, and average values of the daily expansion, daily fire line, speed, and direction of spread (Fig. 1, Table A1). In addition, gridded 500 m global maps of the Global Fire Atlas adjusted burn dates, daily fire line, speed and direction of spread are available in GeoTIFF format. A monthly gridded product is also available at 0.25° resolution. Global Fire Atlas data products can also be visualized and evaluated using an online tool at globalfiredata.org to explore individual fire characteristics for a selected region of interest.

6 Conclusions

The Global Fire Atlas is a new publicly available global dataset on seven key fire characteristics: ignition location and timing, fire size, duration, daily expansion, daily fire line, speed, and direction of spread. Over the 2003 – 2016 study period, we identified 13,250,145 individual fires (≥ 21 ha) based on the moderate resolution MCD64A1 collection 6 burned area data. Striking differences were observed among global fire regimes along gradients of ecosystem productivity and human land use. In general, in ecosystems of abundant fuel and low human influence, large fires of long duration dominated total burned

area, with large numbers of small fires contributing most to overall burned area in human-dominated regions or areas too wet for frequent fires. Fires moved quickly through arid ecosystems with low fuel densities but fire sizes were eventually limited by fuels from natural or human landscape fragmentation. The dataset enables new lines of investigation for understanding vegetation-fire feedbacks, climatic and human controls on global burned area, fire forecasting, emissions modeling, and benchmarking of global fire models.

Appendix A: Supporting material for the methods

Table A1: Overview of the Global Fire Atlas data-layers. The shapefiles of ignition locations (point) and fire perimeters (polygon) contain attribute tables with summary information for each individual fire, while the underlying 500 m gridded layers reflect the day-to-day behavior of the individual fires. In addition, we provide aggregate monthly layers at 0.25° resolution for regional and global analyses.

	Shapefile attributes*	**500 m daily gridded**	**0.25° monthly gridded**
Ignitions	location and timing	-	sum
Perimeter (km)	per fire	-	-
Size (km^2)	per fire	-	average
Duration (days)	per fire	-	average
Daily fire line (km)	average per fire	yes	average
Daily fire expansion (km^2 day^{-1})	average per fire	-	average
Speed (km day^{-1})	average per fire	yes	average
Direction of spread (-)	dominant per fire	yes	dominant
Day of burn	-	yes	-

* vector data are derived from the underlying 500 m MODIS data.

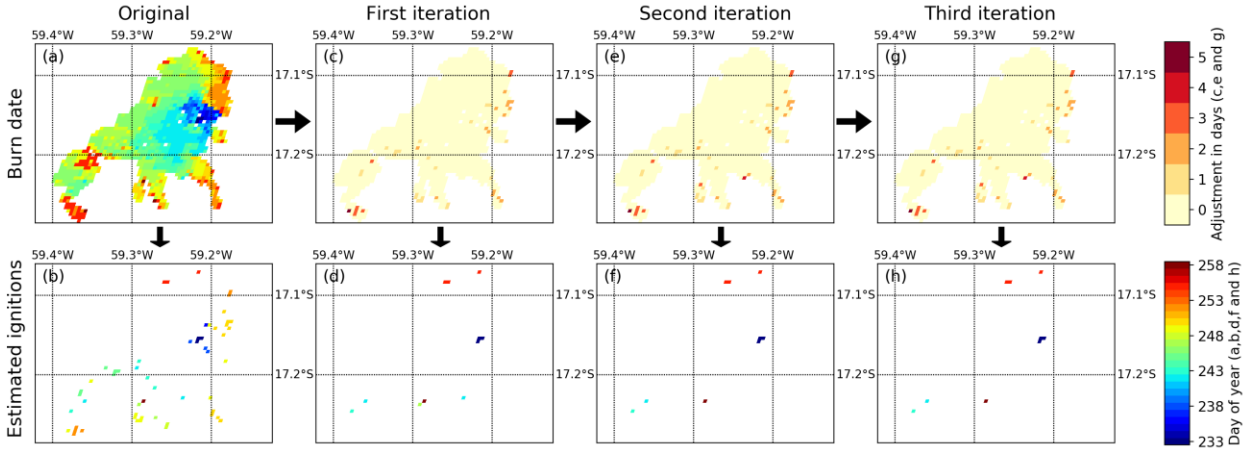

Figure A1: Burn date adjustment to remove local minima that are not associated with ignition points. (a) MCD64A1 burn date estimate for the 2015 example fires in the Cerrado, (b) local minima within (a). (c) Burn date adjustment after the first iteration, and (d) resulting local minima. (e) Burn date adjustment after the second iteration, and (f) resulting local minima. (g) Burn date adjustment after the third iteration, and (h) resulting local minima. Note that for these particular fires there was no difference between (e and f) and (g and h), and the final iteration has no added value here. We found that multiple iterations were particularly beneficial for slow moving fires in forested ecosystems.

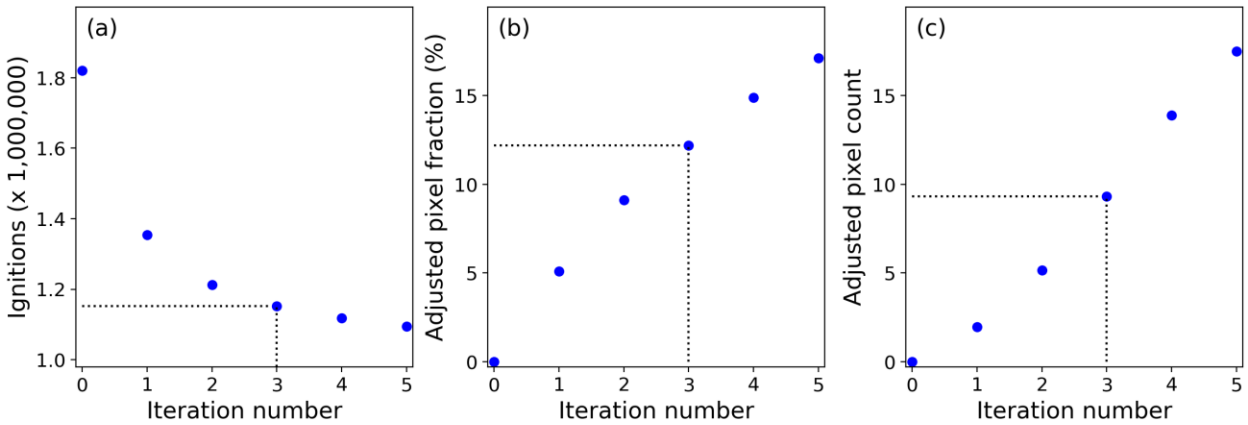

Figure A2: Tradeoffs between reducing local minima not associated with ignition locations and adjustments made to the global burned area product. (a) Local minima (ignitions) detected within the daily 500 m global burned area data for 2015 after different number of iterations of the ignition point filter, (b) corresponding fraction of burned area pixels with adjusted burn date, and (c) corresponding number of burned area pixels adjusted divided by the reduction in ignition count. In this study, we used three iterations of the ignition point filter (indicated with the intermittent lines in figures a, b and c), and "0 iterations" refers to the original MCD64A1 col. 6 burned area data.

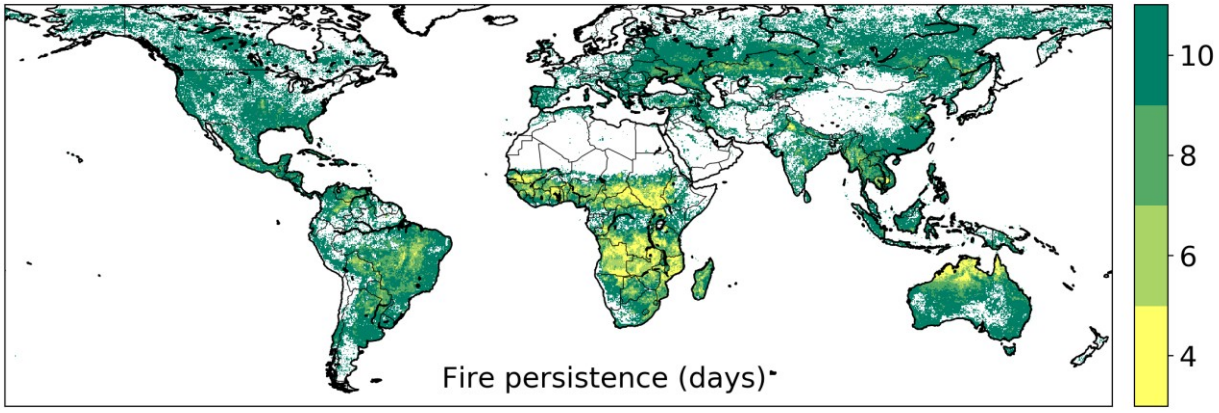

Figure ~~A2~~A3: Average fire persistence threshold at 0.25° resolution. The fire persistence threshold determines how long a fire may take to spread from one 500 m grid cell into the next. We used a 4-day fire persistence threshold for 500 m grid cells that burned more than 3 times during the study period (2003 - 2016), and a 6, 8 and 10-day fire persistence period for grid cells that burned 2-3, 1-2, or 1 time, respectively.

Appendix B: Supporting material for the results and discussion

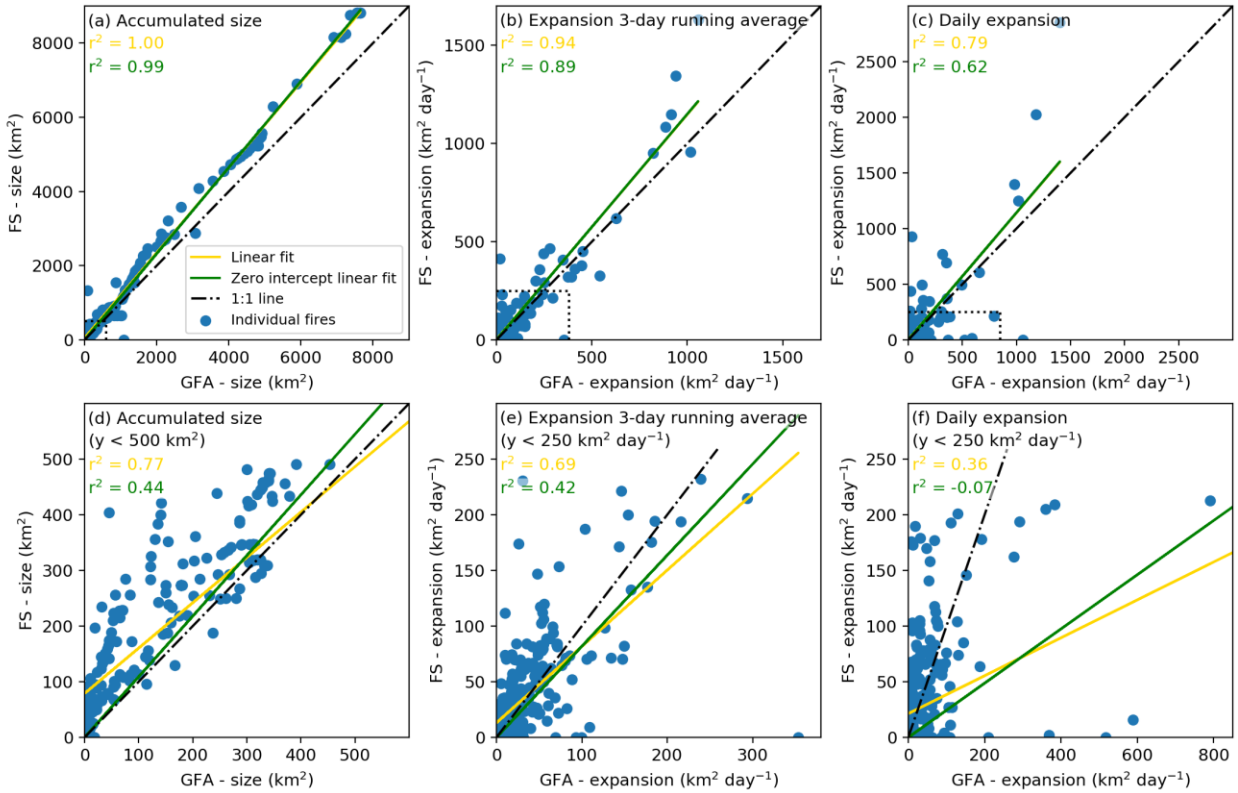

Figure B1: Comparison of daily Global Fire Atlas and US Forest Service data for a selected number of well characterized wildfires in the US. (a) The accumulated daily fire size (for all fires, N=15) illustrates the ability of the Global Fire Atlas to reproduce individual large fire sizes at any specific day over the fire lifetime (each blue dot indicates the size of a specific fire on a specific day). (b) A 3-day running average of the daily growth or "expansion" of each fire (km^2 day^{-1}) and (c) the daily expansion on each day of each fire. Figures (d), (e), and (f) are like (a), (b), and (c), but for US Forest Service fire sizes smaller than 500 km^2 or expansion rates lower than 250 km^2 day^{-1} and corresponding Global Fire Atlas estimates (see intermittent boxes on top-figures).

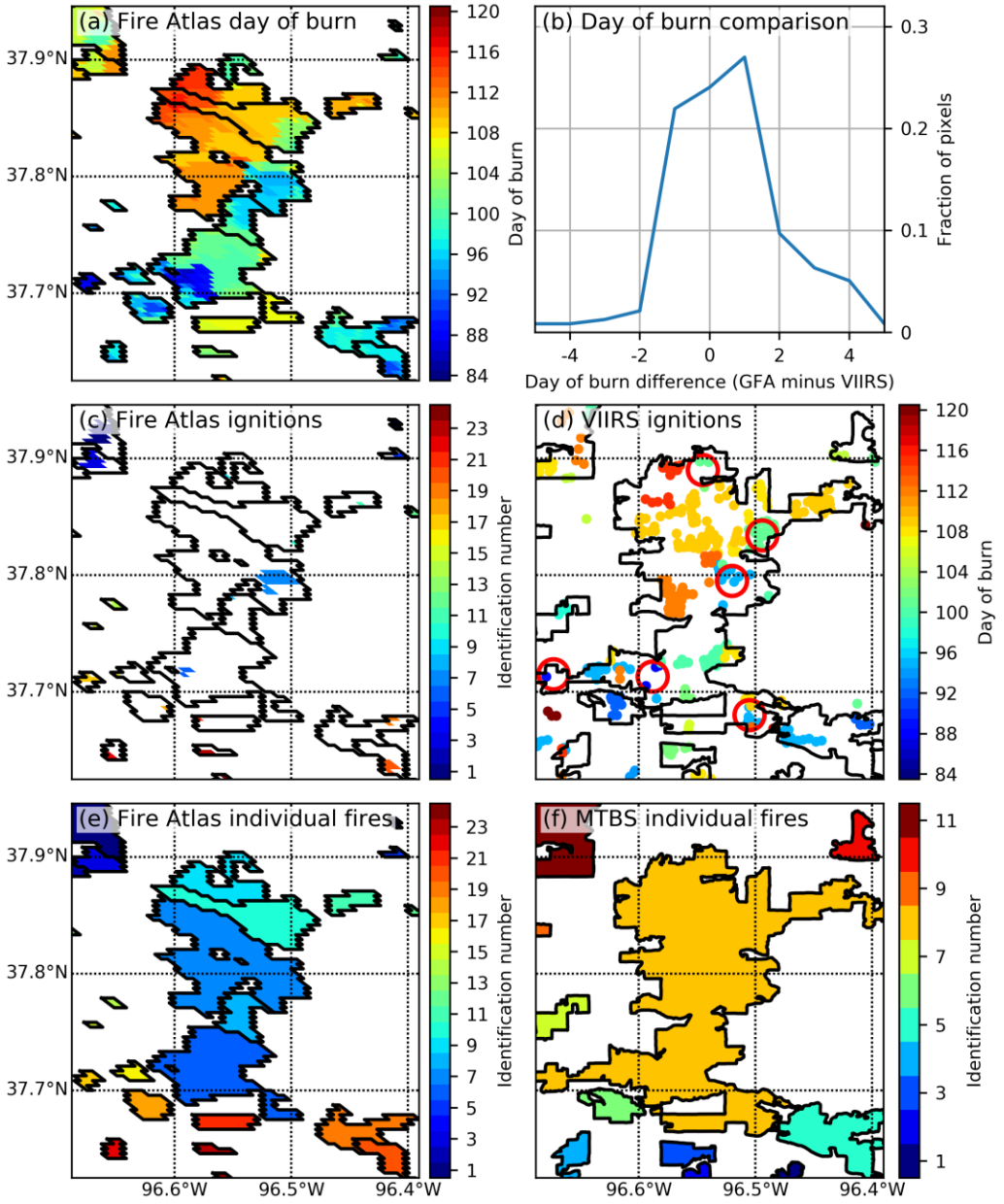

Figure B2: Comparison of Global Fire Atlas ~~and MTBS~~ perimeters and ignition locations to estimates based on MTBS and VIIRS for frequently-burning grasslands in Kansas, USA. (a) Global Fire Atlas adjusted burn dates from MCD64A1, (b) per-pixel comparison of adjusted burn dates used within the Global Fire Atlas (GFA) to the day of the (first) active fire detection from VIIRS, (c) ignition points as estimated by the Global Fire Atlas, (d) manually interpreted ignition locations (red circles) based on VIIRS active fire detections on top of MTBS fire perimeters, (e) individual fires as estimated by the Global Fire Atlas, and (~~e~~f) the MTBS burned area and individual fires ~~and (d) individual fires as estimated by the Global Fire Atlas~~. Here, MCD64A1 data underestimates the total burned area compared to the visual interpretation of Landsat data within the MTBS project, resulting in fragmentation of individual large fires. However, the daily temporal resolution of MODIS imagery allows the Global Fire Atlas to distinguish individual fires and ignition points within larger burn scars that cannot be resolved from infrequent Landsat observations used to delineate fire perimeters within the MTBS project. Broad patterns of ignition locations identified by the Global Fire Atlas are confirmed by manual interpretation of patterns inferred from VIIRS active fire detections (d).

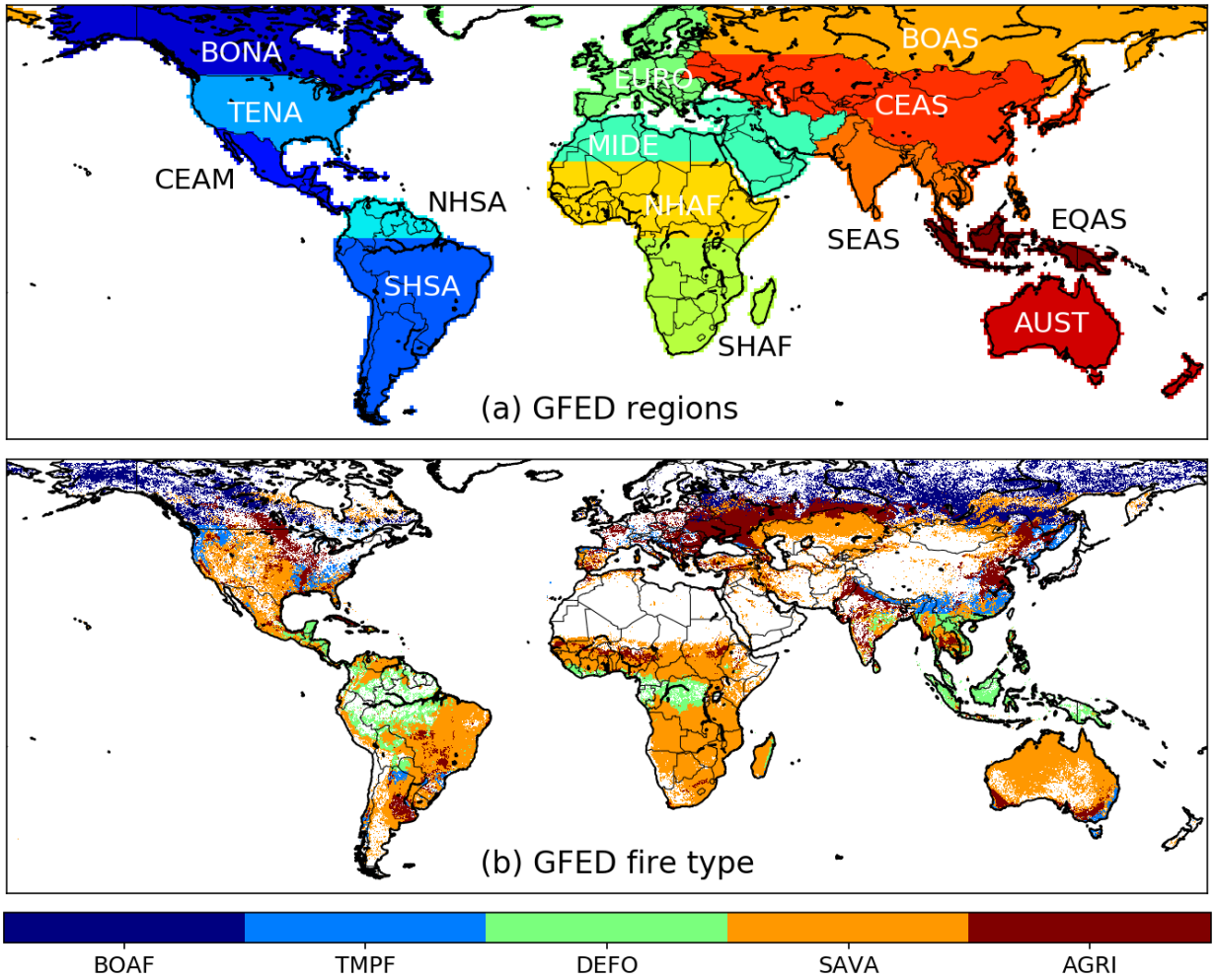

Figure ~~B2~~B3: Global Fire Emissions Database (GFED) regions and dominant GFED fire types used for Tables 1 and 2. (a) GFED regions used in Table 1, and (b) GFED dominant fire type as used in Table 2. Abbreviations of the GFED regions shown in (a) are: boreal North America (BONA), temperate North America (TENA), Central America (CEAM), northern hemisphere South America (NHSA), southern hemisphere South America (SHSA), Europe (EURO), Middle East (MIDE), northern hemisphere Africa (NHAF), southern hemisphere Africa (SHAF), boreal Asia (BOAS), Central Asia (CEAS) southeast Asia (SEAS), equatorial Asia (EQAS), and Australia and New Zealand (AUST). Abbreviations of the GFED fire types shown in (b) are: boreal forests (BOAF), Temperate forests (TMPF), Tropical forest deforestation (DEFO), savanna (SAVA) and agriculture (AGRI).

Author contributions. NA, DCM, and JTR designed the study. NA carried out the data processing and analysis. All authors contributed to the interpretation of the results and writing of the manuscript.

Competing interests. The authors declare that they have no conflict of interest.

Acknowledgements. This work was supported by NASA's Carbon Monitoring System program (grant 80NSSC18K0179) and the Gordon and Betty Moore Foundation (grant GBMF3269). We thank Thomas Mellin of the USFS for granting access to the daily fire perimeter collected over the western USA.

References

Abreu, R. C. R., Hoffmann, W. A., Vasconcelos, H. L., Pilon, N. A., Rossatto, D. R. and Durigan, G.: The biodiversity cost of carbon sequestration in tropical savanna, Sci. Adv., 3, e1701284, doi:10.1126/sciadv.1701284, 2017.

Alencar, A., Asner, G. P., Knapp, D. and Zarin, D.: Temporal variability of forest fires in eastern Amazonia., Ecol. Appl., 21, 2397–2412, doi:10.1890/10-1168.1, 2011.

Andela, N., Kaiser, J. W., van der Werf, G. R. and Wooster, M. J.: New fire diurnal cycle characterizations to improve fire radiative energy assessments made from MODIS observations, Atmos. Chem. Phys., 15, 8831–8846, doi:10.5194/acp-15-8831-2015, 2015.

Andela, N., Morton, D. C., Giglio, L., Chen, Y., Van Der Werf, G. R., Kasibhatla, P. S., Defries, R. S., Collatz, G. J., Hantson, S., Kloster, S., Bachelet, D., Forrest, M., Lasslop, G., Li, F., Mangeon, S., Melton, J. R., Yue, C. and Randerson, J. T.: A human-driven decline in global burned area, Science, 356, 1356–1362, doi:10.1126/science.aal4108, 2017.

Aragão, L. E. O. C., Anderson, L. O., Fonseca, M. G., Rosan, T. M., Vedovato, L. B., Wagner, F. H., Silva, C. V. J., Silva Junior, C. H. L., Arai, E., Aguiar, A. P., Barlow, J., Berenguer, E., Deeter, M. N., Domingues, L. G., Gatti, L., Gloor, M., Malhi, Y., Marengo, J. A., Miller, J. B., Phillips, O. L. and Saatchi, S.: 21st Century drought-related fires counteract the decline of Amazon deforestation carbon emissions, Nat. Commun., 9, 536, doi:10.1038/s41467-017-02771-y, 2018.

Archibald, S., Lehmann, C. E. R., Gómez-Dans, J. L. and Bradstock, R. A.: Defining pyromes and global syndromes of fire regimes, Proc. Natl. Acad. Sci. U. S. A., 110, 6442–6447, doi:10.1073/pnas.1211466110, 2013.

Archibald, S. and Roy, D. P.: Identifying individual fires from satellite-derived burned area data, IEEE Int. Geosci. Remote Sens. Symp. Proc., 9, 160–163, doi:10.1109/IGARSS.2009.5417974, 2009.

Archibald, S., Staver, A. C. and Levin, S. A.: Evolution of human-driven fire regimes in Africa, Proc. Natl. Acad. Sci., 109, 847–852, doi:10.1073/pnas.1118648109, 2012.

Balch, J. K., Bradley, B. A., Abatzoglou, J. T., Nagy, R. C., Fusco, E. J. and Mahood, A. L.: Human-started wildfires expand the fire niche across the United States, Proc. Natl. Acad. Sci. U. S. A., 114, 2946–2951, doi:10.1073/pnas.1617394114, 2017.

Bauters, M., Drake, T. W., Verbeeck, H., Bodé, S., Hervé-Fernández, P., Zito, P., Podgorski, D. C., Boyemba, F., Makelele, I., Cizungu Ntaboba, L., Spencer, R. G. M. and Boeckx, P.: High fire-derived nitrogen deposition on central African forests, Proc. Natl. Acad. Sci. U. S. A., 115, 549–554, doi:10.1073/pnas.1714597115, 2018.

Benali, A., Russo, A., Sá, A. C. L., Pinto, R. M. S., Price, O., Koutsias, N. and Pereira, J. M. C.: Determining fire dates and locating ignition points with satellite data, Remote Sens., 8, 326, doi:10.3390/rs8040326, 2016.

Bond, W. J., Woodward, F. I. and Midgley, G. F.: The global distribution of ecosystems in a world without fire, New Phytol., 165, 525–537, doi:10.1111/j.1469-8137.2004.01252.x, 2005.

Boschetti, L., Roy, D. P. and Justice, C. O.: International Global Burned Area Satellite Product Validation Protocol. In: CEOS-CalVal (Ed.), Part I–production and standardization of validation reference data, Commitee Earth Obs. Satell. USA, pp. 1-11, 2009.

Bowman, D. M. J. S., Balch, J. K., Artaxo, P., Bond, W. J., Carlson, J. M., Cochrane, M. A., D'Antonio, C. M., Defries, R. S., Doyle, J. C., Harrison, S. P., Johnston, F. H., Keeley, J. E., Krawchuk, M. A., Kull, C. A., Marston, J. B., Moritz, M. A., Prentice, I. C., Roos, C. I., Scott, A. C., Swetnam, T. W., van der Werf, G. R. and Pyne, S. J.: Fire in the Earth system, Science, 324, 481–484,

doi:10.1126/science.1163886, 2009.

Brando, P. M., Balch, J. K., Nepstad, D. C., Morton, D. C., Putz, F. E., Coe, M. T., Silvério, D., Macedo, M. N., Davidson, E. A., Nóbrega, C. C., Alencar, A. and Soares-Filho, B. S.: Abrupt increases in Amazonian tree mortality due to drought-fire interactions., Proc. Natl. Acad. Sci. U. S. A., 111, 6347–6352, doi:10.1073/pnas.1305499111, 2014.

Chen, Y., Morton, D. C., Andela, N., Van Der Werf, G. R., Giglio, L. and Randerson, J. T.: A pan-tropical cascade of fire driven by El Niño/Southern Oscillation, Nat. Clim. Chang., 7, 906–911, doi:10.1038/s41558-017-0014-8, 2017.

Coen, J. L. and Schroeder, W.: Use of spatially refined satellite remote sensing fire detection data to initialize and evaluate coupled weather-wildfire growth model simulations, Geophys. Res. Lett., 40, 5536–5541, doi:10.1002/2013GL057868, 2013.

Earl, N. and Simmonds, I.: Spatial and Temporal Variability and Trends in 2001–2016 Global Fire Activity, J. Geophys. Res. Atmos., 123, 2524–2536, doi:10.1002/2017JD027749, 2018.

Eidenshink, J., Schwind, B., Brewer, K., Zhu, Z.-L., Quayle, B. and Howard, S.: A Project for Monitoring Trends in Burn Severity, Fire Ecol., 3, 3–21, doi:10.4996/fireecology.0301003, 2007.

Field, R. D., Werf, G. R. Van Der, Fanin, T., Fetzer, E. J., Fuller, R., Jethva, H., Levy, R., van der Werf, G. R., Fanin, T., Fetzer, E. J., Fuller, R., Jethva, H., Levy, R., Livesey, N. J., Luo, M., Torres, O. and Worden, H. M.: Indonesian fire activity and smoke pollution in 2015 show persistent nonlinear sensitivity to El Niño-induced drought, Proc. Natl. Acad. Sci. U. S. A., 113, 9204–9209, doi:10.1073/pnas.1524888113, 2016.

Frantz, D., Stellmes, M., Röder, A. and Hill, J.: Fire spread from MODIS burned area data: Obtaining fire dynamics information for every single fire, Int. J. Wildl. Fire, 25, 1228–1237, doi:10.1071/WF16003, 2016.

Freeborn, P. H., Wooster, M. J. and Roberts, G.: Addressing the spatiotemporal sampling design of MODIS to provide estimates of the fire radiative energy emitted from Africa, Remote Sens. Environ., 115, 475–489, doi:10.1016/j.rse.2010.09.017, 2011.

Friedl, M. A., McIver, D. K., Hodges, J. C. F., Zhang, X. Y., Muchoney, D., Strahler, A. H., Woodcock, C. E., Gopal, S., Schneider, A., Cooper, A., Baccini, A., Gao, F. and Schaaf, C.: Global land cover mapping from MODIS: algorithms and early results, Remote Sens. Environ., 83, 287–302, doi:10.1016/S0034-4257(02)00078-0, 2002.

Fusco, E. J., Abatzoglou, J. T., Balch, J. K., Finn, J. T. and Bradley, B. A.: Quantifying the human influence on fire ignition across the western USA, Ecol. Appl., 26, 2388–2399, doi:10.1002/eap.1395, 2016.

Fusco, E. J., Finn, J. T., Abatzoglou, J. T., Balch, J. K., Dadashi, S. and Bradley, B. A.: Detection rates and biases of fire observations from MODIS and agency reports in the conterminous United States, Remote Sens. Environ., 220, 30–40, doi:10.1016/j.rse.2018.10.028, 2019.

Giglio, L., Boschetti, L., Roy, D. P., Humber, M. L. and Justice, C. O.: The Collection 6 MODIS burned area mapping algorithm and product, Remote Sens. Environ., 217(July), 72–85, doi:10.1016/j.rse.2018.08.005, 2018.

Giglio, L., Loboda, T., Roy, D. P., Quayle, B. and Justice, C. O.: An active-fire based burned area mapping algorithm for the MODIS sensor, Remote Sens. Environ., 113, 408–420, doi:10.1016/j.rse.2008.10.006, 2009.

Giglio, L., Randerson, J. T. and van der Werf, G. R.: Analysis of daily, monthly, and annual burned area using the fourth-generation global fire emissions database (GFED4), J. Geophys. Res. Biogeosciences,

118, 317–328, doi:10.1002/jgrg.20042, 2013.

Di Giuseppe, F., Rémy, S., Pappenberger, F. and Wetterhall, F.: Using the Fire Weather Index (FWI) to improve the estimation of fire emissions from fire radiative power (FRP) observations, Atmos. Chem. Phys., 18, 5359–5370, doi:10.5194/acp-18-5359-2018, 2018.

Hantson, S., Arneth, A., Harrison, S. P., Kelley, D. I., Prentice, I. C., Rabin, S. S., Archibald, S., Mouillot, F., Arnold, S. R., Artaxo, P., Bachelet, D., Ciais, P., Forrest, M., Friedlingstein, P., Hickler, T., Kaplan, J. O., Kloster, S., Knorr, W., Lasslop, G., Li, F., Mangeon, S., Melton, J. R., Meyn, A., Sitch, S., Spessa, A., van der Werf, G. R., Voulgarakis, A. and Yue, C.: The status and challenge of global fire modelling, Biogeosciences, 13, 3359–3375, doi:10.5194/bg-2016-17, 2016.

Hantson, S., Pueyo, S. and Chuvieco, E.: Global fire size distribution is driven by human impact and climate, Glob. Ecol. Biogeogr., 24, 77–86, doi:10.1111/geb.12246, 2015.

Hantson, S., Scheffer, M., Pueyo, S., Xu, C., Lasslop, G., Van Nes, E. H., Holmgren, M. and Mendelsohn, J.: Rare, Intense, Big fires dominate the global tropics under drier conditions, Sci. Rep., 7, 14374, doi:10.1038/s41598-017-14654-9, 2017.

Humber, M. L., Boschetti, L., Giglio, L. and Justice, C. O.: Spatial and temporal intercomparison of four global burned area products, Int. J. Digit. Earth, 8947, 1–25, doi:10.1080/17538947.2018.1433727, 2018.

Johnston, F. H., Henderson, S. B., Chen, Y., Randerson, J. T., Marlier, M., Defries, R. S., Kinney, P., Bowman, D. M. J. S. and Brauer, M.: Estimated global mortality attributable to smoke from landscape fires, Environ. Health Perspect., 120, 695–701, doi:10.1289/ehp.1104422, 2012.

Jolly, W. M., Cochrane, M. A., Freeborn, P. H., Holden, Z. A., Brown, T. J., Williamson, G. J. and Bowman, D. M. J. S.: Climate-induced variations in global wildfire danger from 1979 to 2013, Nat. Commun., 6, 7537, doi:10.1038/ncomms8537, 2015.

Kaiser, J. W., Heil, A., Andreae, M. O., Benedetti, A., Chubarova, N., Jones, L., Morcrette, J. J., Razinger, M., Schultz, M. G., Suttie, M. and van der Werf, G. R.: Biomass burning emissions estimated with a global fire assimilation system based on observed fire radiative power, Biogeosciences, 9(1), 527–554, doi:10.5194/bg-9-527-2012, 2012.

Kasischke, E. S. and Turetsky, M. R.: Recent changes in the fire regime across the North American boreal region - Spatial and temporal patterns of burning across Canada and Alaska, Geophys. Res. Lett., 33, L09703, doi:10.1029/2006GL025677, 2006.

Knorr, W., Arneth, A. and Jiang, L.: Demographic controls of future global fire risk, Nat. Clim. Chang., 6, 781–785, doi:10.1038/nclimate2999, 2016.

Koplitz, S. N., Mickley, L. J., Marlier, M. E., Buonocore, J. J., Kim, P. S., Liu, T., Sulprizio, M. P., DeFries, R. S., Jacob, D. J., Schwartz, J., Pongsiri, M. and Myers, S. S.: Public health impacts of the severe haze in Equatorial Asia in September-October 2015: Demonstration of a new framework for informing fire management strategies to reduce downwind smoke exposure, Environ. Res. Lett., 11, 094023, doi:10.1088/1748-9326/11/9/094023, 2016.

Laurent, P., Mouillot, F., Yue, C., Ciais, P., Moreno, M. V. and Nogueira, J. M. P.: FRY, a global database of fire patch functional traits derived from space-borne burned area products, Sci. Data, 5, 180132, doi:10.1038/sdata.2018.132, 2018.

Van Leeuwen, T. T. and Van Der Werf, G. R.: Spatial and temporal variability in the ratio of trace gases emitted from biomass burning, Atmos. Chem. Phys., 11, 3611–3629, doi:10.5194/acp-11-3611-2011, 2011.

Lelieveld, J., Evans, J. S., Fnais, M., Giannadaki, D. and Pozzer, A.: The contribution of outdoor air pollution sources to premature mortality on a global scale, Nature, 525, 367–371,

doi:10.1038/nature15371, 2015.

Loboda, T. V. and Csiszar, I. A.: Reconstruction of fire spread within wildland fire events in Northern Eurasia from the MODIS active fire product, Glob. Planet. Change, 56, 258–273, doi:10.1016/j.gloplacha.2006.07.015, 2007.

Moritz, M. A., Batllori, E., Bradstock, R. A., Gill, A. M., Handmer, J., Hessburg, P. F., Leonard, J., McCaffrey, S., Odion, D. C., Schoennagel, T. and Syphard, A. D.: Learning to coexist with wildfire, Nature, 515, 58–66, doi:10.1038/nature13946, 2014.

Morton, D. C., Collatz, G. J., Wang, D., Randerson, J. T., Giglio, L. and Chen, Y.: Satellite-based assessment of climate controls on US burned area, Biogeosciences, 10, 247–260, doi:10.5194/bg-10-247-2013, 2013a.

Morton, D. C., Page, Y. Le, Defries, R., Collatz, G. J. and Hurtt, G. C.: Understorey fire frequency and the fate of burned forests in southern Amazonia, Phil. Trans. R. Soc. B, 368, 20120163, doi:10.1098/rstb.2012.0163, 2013b.

Nogueira, J. M. P., Ruffault, J., Chuvieco, E. and Mouillot, F.: Can we go beyond burned area in the assessment of global remote sensing products with fire patch metrics?, Remote Sens., 9, 7, doi:10.3390/rs9010007, 2017.

Oom, D., Silva, P. C., Bistinas, I. and Pereira, J. M. C.: Highlighting biome-specific sensitivity of fire size distributions to time-gap parameter using a new algorithm for fire event individuation, Remote Sens., 8, 663, doi:10.3390/rs8080663, 2016.

Padilla, M., Stehman, S. V., Ramo, R., Corti, D., Hantson, S., Oliva, P., Alonso-Canas, I., Bradley, A. V., Tansey, K., Mota, B., Pereira, J. M. and Chuvieco, E.: Comparing the accuracies of remote sensing global burned area products using stratified random sampling and estimation, Remote Sens. Environ., 160, 114–121, doi:10.1016/j.rse.2015.01.005, 2015.

Le Page, Y., Morton, D., Bond-Lamberty, B., Pereira, J. M. C. and Hurtt, G.: HESFIRE: A global fire model to explore the role of anthropogenic and weather drivers, Biogeosciences, 12, 887–903, doi:10.5194/bg-12-887-2015, 2015.

Parker, R. J., Boesch, H., Wooster, M. J., Moore, D. P., Webb, A. J., Gaveau, D. and Murdiyarso, D.: Atmospheric CH4 and CO2 enhancements and biomass burning emission ratios derived from satellite observations of the 2015 Indonesian fire plumes, Atmos. Chem. Phys., 16, 10111–10131, doi:10.5194/acp-16-10111-2016, 2016.

Pellegrini, A. F. A., Ahlström, A., Hobbie, S. E., Reich, P. B., Nieradzik, L. P., Staver, A. C., Scharenbroch, B. C., Jumpponen, A., Anderegg, W. R. L., Randerson, J. T. and Jackson, R. B.: Fire frequency drives decadal changes in soil carbon and nitrogen and ecosystem productivity, Nature, 53, 194–198, doi:10.1038/nature24668, 2018.

Pfeiffer, M., Spessa, A. and Kaplan, J. O.: A model for global biomass burning in preindustrial time: LPJ-LMfire (v1.0), Geosci. Model Dev., 6, 643–685, doi:10.5194/gmd-6-643-2013, 2013.

Rabin, S. S., Melton, J. R., Lasslop, G., Bachelet, D., Forrest, M., Hantson, S., Kaplan, J. O., Li, F., Mangeon, S., Ward, D. S., Yue, C., Arora, V. K., Hickler, T., Kloster, S., Knorr, W., Nieradzik, L., Spessa, A., Folberth, G. A., Sheehan, T., Voulgarakis, A., Kelley, D. I., Colin Prentice, I., Sitch, S., Harrison, S. and Arneth, A.: The Fire Modeling Intercomparison Project (FireMIP), phase 1: Experimental and analytical protocols with detailed model descriptions, Geosci. Model Dev., 10, 1175–1197, doi:10.5194/gmd-10-1175-2017, 2017.

Randerson, J. T., Chen, Y., van der Werf, G. R., Rogers, B. M. and Morton, D. C.: Global burned area and biomass burning emissions from small fires, J. Geophys. Res., 117, G04012, doi:10.1029/2012JG002128, 2012.

Randerson, J. T., Liu, H., Flanner, M. G., Chambers, S. D., Jin, Y., Hess, P. G., Pfister, G., Mack, M. C., Treseder, K. K., Welp, L. R., Chapin, F. S., Harden, J. W., Goulden, M. L., Lyons, E., Neff, J. C., Schuur, E. A. G. and Zender, C. S.: The impact of boreal forest fire on climate warming, Science, 314, 1130–1132, doi:10.1126/science.1132075, 2006.

Reisen, F., Meyer, C. P., Weston, C. J. and Volkova, L.: Ground-based Field Measurements of $PM_{2.5}$ Emission Factors from Flaming and Smouldering Combustion in Eucalypt Forests, J. Geophys. Res. Atmos., doi:10.1029/2018JD028488, 2018.

Roteta, E., Bastarrika, A., Padilla, M., Storm, T. and Chuvieco, E.: Development of a Sentinel-2 burned area algorithm: Generation of a small fire database for sub-Saharan Africa, Remote Sens. Environ., 222(September 2017), 1–17, doi:10.1016/j.rse.2018.12.011, 2019.

Sá, A. C. L., Benali, A., Fernandes, P. M., Pinto, R. M. S., Trigo, R. M., Salis, M., Russo, A., Jerez, S., Soares, P. M. M., Schroeder, W. and Pereira, J. M. C.: Evaluating fire growth simulations using satellite active fire data, Remote Sens. Environ., 190, 302–317, doi:10.1016/j.rse.2016.12.023, 2017.

Scholes, R. J. and Archer, S. R.: Tree-grass interactions in savannas, Annu. Rev. Ecol. Syst., 28, 517–544, doi:10.1146/annurev.ecolsys.28.1.517, 1997.

Schroeder, W., Oliva, P., Giglio, L. and Csiszar, I. A.: The New VIIRS 375m active fire detection data product: Algorithm description and initial assessment, Remote Sens. Environ., 143, 85–96, doi:10.1016/j.rse.2013.12.008, 2014.

Schroeder, W., Prins, E., Giglio, L., Csiszar, I., Schmidt, C., Morisette, J. and Morton, D.: Validation of GOES and MODIS active fire detection products using ASTER and ETM+ data, Remote Sens. Environ., 112, 2711–2726, doi:10.1016/j.rse.2008.01.005, 2008.

Sparks, A. M., Boschetti, L., Smith, A. M. S., Tinkham, W. T., Lannom, K. O. and Newingham, B. A.: An accuracy assessment of the MTBS burned area product for shrub-steppe fires in the northern Great Basin, United States, Int. J. Wildl. Fire, 24, 70–78, doi:10.1071/WF14131, 2015.

Staver, A. C., Archibald, S. and Levin, S. A.: The Global Extent and Determinants of Savanna and Forest as Alternative Biome States, Science, 334, 230–232, doi:10.1126/science.1210465, 2011.

Taylor, A. H., Trouet, V., Skinner, C. N. and Stephens, S.: Socioecological transitions trigger fire regime shifts and modulate fire – climate interactions in the Sierra, Proc. Natl. Acad. Sci. U. S. A., 113, 13684–13689, doi:10.1073/pnas.1609775113, 2016.

Thonicke, K., Spessa, A., Prentice, I. C., Harrison, S. P., Dong, L. and Carmona-Moreno, C.: The influence of vegetation, fire spread and fire behaviour on biomass burning and trace gas emissions: results from a process-based model, Biogeosciences, 7, 1991–2011, doi:10.5194/bg-7-1991-2010, 2010.

Veraverbeke, S., Sedano, F., Hook, S. J., Randerson, J. T., Jin, Y. and Rogers, B. M.: Mapping the daily progression of large wildland fires using MODIS active fire data, Int. J. Wildl. Fire, 23, 655–667, doi:10.1071/WF13015, 2014.

Ward, D. S., Kloster, S., Mahowald, N. M., Rogers, B. M., Randerson, J. T. and Hess, P. G.: The changing radiative forcing of fires: global model estimates for past, present and future, Atmos. Chem. Phys., 12, 10857–10886, doi:10.5194/acp-12-10857-2012, 2012.

Ward, D. S., Shevliakova, E., Malyshev, S. and Rabin, S.: Trends and Variability of Global Fire Emissions Due To Historical Anthropogenic Activities, Global Biogeochem. Cycles, 32, 122–142, doi:10.1002/2017GB005787, 2018.

van der Werf, G. R., Dempewolf, J., Trigg, S. N., Randerson, J. T., Kasibhatla, P. S., Giglio, L., Murdiyarso, D., Peters, W., Morton, D. C., Collatz, G. J., Dolman, A. J. and DeFries, R. S.: Climate regulation of fire emissions and deforestation in equatorial Asia., Proc. Natl. Acad. Sci. U. S. A., 105,

20350–20355, doi:10.1073/pnas.0803375105, 2008.

Westerling, A. L., Hidalgo, H. G., Cayan, D. R. and Swetnam, T. W.: Warming and earlier spring increase western US forest wildfire activity, Science, 313, 940–943, doi:10.1126/science.1128834, 2006.

Yang, J., Tian, H., Tao, B., Ren, W., Pan, S., Liu, Y. and Wang, Y.: A growing importance of large fires in conterminous United States during 1984-2012, J. Geophys. Res. Biogeosciences, 120, 2625–2640, doi:10.1002/2015JG002965, 2015.

Young, A. M., Higuera, P. E., Duffy, P. A. and Hu, F. S.: Climatic thresholds shape northern high-latitude fire regimes and imply vulnerability to future climate change, Ecography, 40, 606–617, doi:10.1111/ecog.02205, 2017.